

## Differential sensory and immune gene evolution in sea turtles with contrasting demographic and life histories

Blair P. Bentley<sup>1,†</sup>, Tomás Carrasco-Valenzuela<sup>2,3</sup>, Elisa K. S. Ramos<sup>2,3,4</sup>, Harvinder Pawar<sup>5</sup>, Larissa Souza Arantes<sup>2,3</sup>, Alana Alexander<sup>6</sup>, Shreya M. Banerjee<sup>1,7</sup>, Patrick Masterson<sup>8</sup>, Martin Kuhlwiilm<sup>5,9,10</sup>, Martin Pippel<sup>11,12</sup>, Jacquelyn Mountcastle<sup>13,22</sup>, Bettina Haase<sup>13</sup>, Marcela Uliano Silva<sup>2,3</sup>, Giulio Formenti<sup>13,14</sup>, Kerstin Howe<sup>15</sup>, William Chow<sup>15</sup>, Alan Tracey<sup>15</sup>, Yumi Sims<sup>15</sup>, Sarah Pelan<sup>15</sup>, Jonathan Wood<sup>15</sup>, Justin R. Perrault<sup>16</sup>, Kelly Stewart<sup>17</sup>, Scott R. Benson<sup>18,19</sup>, Yaniv Levy<sup>20</sup>, Erica V. Todd<sup>21</sup>, H. Bradley Shaffer<sup>22,23</sup>, Peter Scott<sup>22,24</sup>, Brian T. Henen<sup>25</sup>, Robert W. Murphy<sup>26</sup>, David W. Mohr<sup>27</sup>, Alan F. Scott<sup>27</sup>, Neil J. Gemmell<sup>28</sup>, Alexander Suh<sup>29,30</sup>, Sylke Winkler<sup>11,31</sup>, Françoise Thibaud-Nissen<sup>8</sup>, Mariana F. Nery<sup>4</sup>, Tomas Marques-Bonet<sup>5,32,33,34</sup>, Agostinho Antunes<sup>35,36</sup>, Yaron Tikochinski<sup>37</sup>, Peter H. Dutton<sup>17</sup>, Olivier Fedrigo<sup>13</sup>, Eugene W. Myers<sup>11,12,38</sup>, Erich D. Jarvis<sup>13,14,39</sup>, Camila J. Mazzoni<sup>2,3,\*</sup>, and Lisa M. Komoroske<sup>1,\*</sup>

<sup>1</sup>Department of Environmental Conservation, University of Massachusetts, Amherst, MA, USA; <sup>2</sup>Evolutionary Genetics Department, Leibniz Institute for Zoo and Wildlife Research, Berlin, Germany; <sup>3</sup>Berlin Center for Genomics in Biodiversity Research, Berlin, Germany; <sup>4</sup>Department of Genetics, Evolution, Microbiology and Immunology, University of Campinas, Campinas, Brazil; <sup>5</sup>Institut de Biologia Evolutiva, (CSIC-Universitat Pompeu Fabra), PRBB, Doctor Aiguader 88, Barcelona, Catalonia, Spain; <sup>6</sup>Department of Anatomy, School of Biomedical Sciences, University of Otago, Dunedin, New Zealand; <sup>7</sup>Department of Biology, Stanford University, Stanford CA, USA; <sup>8</sup>National Center for Biotechnology Information, National Library of Medicine, National Institutes of Health, Bethesda, MD, USA; <sup>9</sup>Department of Evolutionary Anthropology, University of Vienna, Vienna, Austria; <sup>10</sup>Human Evolution and Archaeological Sciences (HEAS), University of Vienna, Austria; <sup>11</sup>Max Planck Institute of Molecular Cell Biology and Genetics, Dresden, Germany; <sup>12</sup>Center for Systems Biology, Dresden, Germany; <sup>13</sup>Vertebrate Genome Lab, The Rockefeller University, New York, NY, USA; <sup>14</sup>Laboratory of Neurogenetics of Language, The Rockefeller University, New York, NY, USA; <sup>15</sup>Tree of Life, Wellcome Sanger Institute, Cambridge, CB10 1SA, UK; <sup>16</sup>Loggerhead Marinelifelife Center, Juno Beach, FL, USA; <sup>17</sup>Marine Mammal and Turtle Division, Southwest Fisheries Science Center, National Marine Fisheries Service, National Oceanic and Atmospheric Administration, La Jolla, CA, United States; <sup>18</sup>Marine Mammal and Turtle Division, Southwest Fisheries Science Center, National Marine Fisheries Service, National Oceanic and Atmospheric Administration, Moss Landing, CA, USA; <sup>19</sup>Moss Landing Marine Laboratories, Moss Landing, CA, USA; <sup>20</sup>National Sea Rescue Centre, Israel's Nature and Parks Authority, Mevot Yam, Michmoret, Israel; <sup>21</sup>School of Life and Environmental Sciences, Deakin University, Queenscliff, VIC, Australia; <sup>22</sup>Department of Ecology and Evolutionary Biology, University of California, Los Angeles, CA, USA; <sup>23</sup>La Kretz Center for California Conservation Science, Institute of the Environment and Sustainability, University of California, Los Angeles, CA, USA; <sup>24</sup>Department of Life, Earth, and Environmental Sciences, West Texas A&M University, Canyon, TX, USA; <sup>25</sup>Environmental Affairs, Marine Air Ground Task Force and Training Command, Marine Corps Air Ground Combat Center, Twentynine Palms CA, USA; <sup>26</sup>Centre for Biodiversity, Royal Ontario Museum, Toronto, Ontario, Canada; <sup>27</sup>Genetic Resources Core Facility, McKusick-Nathans Dept of Genetic Medicine, Johns Hopkins University School of Medicine, Baltimore MD 21287, USA; <sup>28</sup>Allan Wilson Centre, Department of Anatomy, University of Otago, Dunedin, New Zealand; <sup>29</sup>School of Biological Sciences, University of East Anglia, Norwich NR4 7TU, UK; <sup>30</sup>Department of Organismal Biology, Evolutionary Biology Centre (EBC), Science for Life Laboratory, Uppsala University, Uppsala, Sweden; <sup>31</sup>DRESDEN concept Genome Center, Dresden, Germany; <sup>32</sup>CNAG-CRG, Centre for Genomic Regulation (CRG), Barcelona Institute of Science and Technology (BIST), Baldiri i Reixac 4, 08028 Barcelona, Spain; <sup>33</sup>Institució Catalana de Recerca i Estudis Avançats (ICREA), Barcelona, Catalonia 08010, Spain; <sup>34</sup>Institut Català de Paleontologia Miquel Crusafont, Universitat Autònoma de Barcelona; <sup>35</sup>CIIMAR/CIMAR, Centro Interdisciplinar de Investigação Marinha e Ambiental, Universidade do Porto, Av. General Norton de Matos, s/n, 4450-208, Porto, Portugal; <sup>36</sup>Departamento de Biologia, Faculdade de Ciências, Universidade do Porto, Rua do Campo Alegre, s/n, 4169-007, Porto, Portugal; <sup>37</sup>Faculty of Marine Sciences, Ruppun Academic Center, Michmoret, Israel; <sup>38</sup>Faculty of Computer Science, Technical University Dresden, Dresden, Germany; <sup>39</sup>Howard Hughes Medical Institute, Chevy Chase, MD, USA.

*Classification:* Genetics and Evolution

*Keywords:* marine turtle; gene evolution; conservation genomics; genetic diversity; demographic history

*Abbreviations:* TE - transposable element; RE - repetitive element; RRC - region of reduced collinearity; FP – Fibropapillomatosis; ROH – runs of homozygosity

<sup>†</sup>Corresponding author: Blair P. Bentley, University of Massachusetts, Amherst USA. Email: [bbentley@umass.edu](mailto:bbentley@umass.edu).

\* These authors contributed equally to the work: Camila J. Mazzoni and Lisa M. Komoroske.

53 **Abstract**

54 Sea turtles represent an ancient lineage of marine vertebrates that evolved from terrestrial ancestors over  
55 100 MYA, yet the genomic basis of the unique physiological and ecological traits enabling these species  
56 to thrive in diverse marine habitats remain largely unknown. Additionally, many populations have  
57 declined drastically due to anthropogenic activities over the past two centuries, and their recovery is a  
58 high global conservation priority. We generated and analyzed high-quality reference genomes for green  
59 (*Chelonia mydas*) and leatherback (*Dermochelys coriacea*) turtles, representing the two extant sea turtle  
60 families (MRCA ~60 MYA). These genomes are highly syntenic and homologous, but localized non-  
61 collinearity was associated with higher copy numbers of immune, zinc-finger, or olfactory receptor (OR)  
62 genes in green turtles, and ORs related to waterborne odorants were greatly expanded in green turtles.  
63 These findings suggest that divergent evolution of these key gene families may underlie immunological  
64 and sensory adaptations assisting navigation, occupancy of neritic versus pelagic environments, and diet  
65 specialization. Reduced collinearity was especially prevalent in microchromosomes, with greater gene  
66 content, heterozygosity, and genetic distances between species, supporting their critical role in vertebrate  
67 evolutionary adaptation. Finally, diversity and demographic histories starkly contrasted between species,  
68 indicating that leatherback turtles have had a low yet stable effective population size and extremely low  
69 diversity compared to other reptiles, and a higher proportion of deleterious variants, reinforcing concern  
70 over their persistence under future climate scenarios. These genomes provide invaluable resources for  
71 advancing our understanding of evolution and conservation best practices in an imperiled vertebrate  
72 lineage.

73

74 **Statement of significance**

75 Sea turtles represent a clade whose populations have undergone recent global declines. We analyzed de  
76 novo genomes for both extant sea turtle families through the Vertebrate Genomes Project to inform their  
77 conservation and evolutionary biology. The highly conserved genomes were largely differentiated by  
78 localized gene-rich regions of divergence, particularly in microchromosomes, suggesting that these  
79 overlooked genomic elements may play key functional roles in sea turtle evolution. We further  
80 demonstrate that dissimilar evolutionary histories impact standing genomic diversity and genetic load,  
81 and are critical to consider when using these metrics to assess adaptive potential and extinction risk.  
82 Examination of these relationships may be important to reveal drivers of adaptation and diversity in sea  
83 turtles and other vertebrates with conserved genome synteny.

## 84 **Introduction**

85           Sea turtles recolonized marine environments over 100 MYA (1, 2) and are now one of the most  
86 widely distributed vertebrate groups on the planet (3). Leatherback turtles (*Dermochelys coriacea*)  
87 represent the only remaining species of the family Dermochelyidae, which diverged from the Cheloniidae  
88 (hard-shelled sea turtles) about 60 MYA (4). Unique morphological (Fig. 1a) and physiological traits  
89 allow leatherback turtles to exploit cool, highly productive pelagic habitats (5, 6), while green turtles  
90 (*Chelonia mydas*) and other hard-shelled chelonid species largely inhabit warmer nearshore habitats  
91 following an early pelagic life stage. Most previous research in this group has focused on organismal and  
92 ecological adaptations (7), but the genomic basis of traits that differentiate or unite these species is not  
93 well understood.

94           Anthropogenic pressures have caused substantial population declines in sea turtles, with  
95 contemporary populations currently representing mere fractions of their historical abundances (8, 9).  
96 Although sea turtles spend most of their life in the ocean, they also exhibit long-distance migrations to  
97 natal rookeries for terrestrial reproduction (7, 10, 11). Consequently, they are threatened by human  
98 activities in both terrestrial and marine environments, including direct harvest of meat and eggs (12),  
99 fisheries bycatch (13), coastal development (14, 15), pollution (16), disease (17), and climate change (18,  
100 19), which is exacerbated by their temperature-dependent mechanism of sex determination (TSD) altering  
101 population dynamics (20, 21). The IUCN lists most sea turtle species as vulnerable or endangered, and  
102 while decades of conservation efforts have fueled positive trends for some populations (22), others  
103 continue to decline (23). In particular, leatherback turtles have undergone extensive declines (>95% in  
104 some populations) over the last century (24–27), including the extirpation of the Malaysian nesting  
105 population (28). Leatherback turtle recovery is also impeded by relatively low hatching success compared  
106 to other sea turtle species (29). In contrast, many green turtle populations have recently increased  
107 following conservation actions (22), but their continued recovery remains threatened by anthropogenic  
108 activities and high incidence of the neoplastic disease fibropapillomatosis (FP) (30).

109           Genomic data have been instrumental in advancing understanding of species' evolutionary  
110 histories and ecological adaptations (31–33), and providing critical information for conservation  
111 management (34–37). However, this research has been hampered in taxa where genomic resources remain  
112 limited. In particular, the lack of high-quality reference genomes, which are essential for accurate  
113 comparative evolutionary analyses (38, 39) and estimates of a wide range of metrics to inform  
114 conservation biology (36, 40), impede this work in many threatened species. An early draft genome for  
115 the green turtle was assembled almost a decade ago (41), and provided important insights into turtle  
116 evolution. However, errors, gaps, and misassemblies in draft genomes can lead to spurious inferences,  
117 potentially masking signals of interest (38, 42). Well-annotated, chromosomal-level reference genomes  
118 can resolve these issues, improving our understanding of genomic underpinnings of ecological and  
119 evolutionary adaptations (39, 43). For example, high-quality genomes with accurate annotations have  
120 enabled examination of gene changes associated with recolonization of the marine environment by  
121 terrestrial vertebrates, including the loss of olfactory receptor (OR) gene families (32, 44). Comparative  
122 genomic analyses also demonstrated adaptive diversity in genes underlying reptilian immunity (45), with  
123 high-quality genomes providing insights into disease susceptibility (33, 46, 47). This is critical for sea  
124 turtles, with diseases such as FP adversely impacting populations across the globe (30), and information  
125 on immune genes key for devising effective conservation strategies (48). The contiguity of high-quality  
126 genomes is also invaluable for conservation-focused analyses, especially runs of homozygosity (ROH)

127 and genetic load that provide insights into population demography and inbreeding depression, and are  
128 difficult to accurately quantify with fragmented, poorly-annotated genomes (49).

129 Here, we assembled chromosome-level reference genomes with species-specific annotations for  
130 leatherback and green turtles as part of the Vertebrate Genomes Project (VGP) to facilitate critical  
131 research centered around sea turtle evolutionary history and conservation. We conducted comparative  
132 analyses to explore the genomic basis of their shared and unique phenotypic traits, and compared their  
133 chromosomal organization, genomic diversity, and demographic histories. These genomes represent two  
134 of the most contiguous reptilian genomes assembled to date, providing invaluable resources for ongoing  
135 investigations into conservation and adaptation for this imperiled vertebrate lineage.

136

## 137 **Results**

### 138 *Genome quality*

139 The reference genomes of the leatherback and green turtles were generated using four genomic  
140 technologies following the VGP pipeline v1.6 (39), with minor modifications (see Methods). A total of  
141 100% of the leatherback and 99.8% of the green turtle assembled sequences were placeable within  
142 chromosomes. The assembled genomes were near full-length (~2.1 GB), with annotations of all 28 known  
143 chromosomes for both species, composed of 11 macrochromosomes (>50 Mb) and 17 microchromosomes  
144 (<50 Mb) (Tables 1 & S1, Fig. S1). These genomes are among the highest quality genomes assembled for  
145 non-avian reptiles to date in terms of both contiguity and completeness (Table S2), with the leatherback  
146 turtle assembly representing the first reptile genome where all scaffolds have been assigned to  
147 chromosomes. Scaffold N50s were high for both genomes (Table 1). We annotated 18,775 protein-coding  
148 genes in leatherback turtle genome and 19,752 in the green turtle (see below for analysis of gene number  
149 differences). Of these, 96.9% and 97.5%, for leatherback and green turtles respectively, were supported  
150 over 95% of their length from experimental evidence and/or high-quality protein models from related  
151 species (see Methods). The number of protein-coding genes falls within the range for other reptilian  
152 genomes (Table S2) and includes 97.7% and 98.2% complete BUSCO copies when using Sauropsida  
153 models for leatherback and green turtles respectively (50), which are similar or higher proportions than all  
154 other assembled reptilian genomes to date (Fig. S2).

155

### 156 *Genome architecture*

157 Despite diverging over 60 million years ago (4), leatherback and green turtles have extremely  
158 high genome synteny and collinearity (Figs. 1b,c, S3, S4). After multiple rounds of manual curation to  
159 correct any artifacts of misassemblies, only a few larger structural rearrangements remained, including  
160 inversions of up to 7 Mb on chromosomes 12, 13, 24 and 28 (Fig. S3). The high collinearity between the  
161 two genomes included near complete end-to-end contiguous synteny for nine out of 28 chromosomes  
162 (Fig. S3). The remaining 19 chromosomes exhibited at least one small region of reduced collinearity  
163 (RRC) between the species, with RRCs representing a total of ~83.4 Mb (~3.9%) and ~110.5 Mb (~5.2%)  
164 of the leatherback and green turtle genome lengths, respectively. Eight chromosomes exhibited small  
165 RRCs (between 0.1–3 Mb), and 11 contained RRCs that were between 3–18 Mb in length (Figs. 2a-d &  
166 Table S3). Analyses of coding regions revealed a similar pattern of high collinearity between the two  
167 species at the gene level (Figs. 1c & S3), particularly within the macrochromosomes that contain more  
168 than 80% of the total length of the genomes.

169 The two genomes displayed similar percentages of repetitive elements (REs; 45.8% and 44.4%,  
170 respectively; Fig. S5 & Table S4), which were almost exclusively transposable elements (TEs; 30.5% and

171 27.4%) and unclassified repeats (14.6% and 16.5%, respectively). While both genomes carry similar  
172 proportions of REs, the leatherback turtle genome exhibited relatively longer TEs across all but two  
173 chromosomes when compared to the green turtle (Fig. S6a). The landscape of TE superfamily  
174 composition over evolutionary time is generally similar between the two species (Fig. S5), and consistent  
175 with other reptiles (51, 52). One striking difference, however, is seen in REs with low Kimura values  
176 (<5%), which appeared at much higher frequency in the leatherback turtle genome (Fig. S5), representing  
177 either relatively recent insertions or reflecting lower mutation rates in this species.

178

### 179 *Gene families and gene functional analysis*

180 Gene function analysis of localized RRCs revealed that most contain genes with higher copy  
181 numbers in the green turtle compared to the leatherback (Fig. 2a-d, Table S3). From the RRCs in the 19  
182 chromosomes that had higher gene copy numbers in the green turtle, ten contained genes associated with  
183 immune system, olfactory reception and/or zinc-finger protein genes. In addition to localized RRCs,  
184 higher gene copy numbers in the green turtle occurred in many gene orthologous groups (orthogroups)  
185 across the entire genome, and generally in variable multicopy genes (Fig. 2f, g). Copy number variation  
186 accounted for most of the nearly one thousand more genes annotated in the green turtle genome relative to  
187 the leatherback (Fig. 2f, g; Table 1). We detected no evidence of collapsed multicopy genes in the  
188 leatherback turtle assembly across multiple analyses (see Methods), supporting this as a biological signal  
189 rather than technical artifact of assembly.

190 Olfactory receptors (ORs) represented the largest orthogroups in both genomes, and differences  
191 in copy numbers were tightly connected to observed RRCs. All OR Class I genes were clustered at the  
192 beginning of chromosome 1, and the green turtle had higher copy numbers in this region (Fig. 2a-d). This  
193 area also contains a cluster of OR Class I genes in at least three additional testudinid species, and is the  
194 only divergent region across the very large chromosome 1 in the turtles analyzed (Fig. S7). In contrast,  
195 OR Class II genes were spread across several chromosomes in both sea turtle species, but again higher  
196 copy numbers in the green turtle were all found within RRCs (Fig. 2b-d). The instability and rapid  
197 evolution of OR gene numbers in turtles is further illustrated in the expansion-contraction analysis of  
198 orthogroups (Fig. 2e, Table S6a-d), which showed that OR Class I genes underwent a modest contraction  
199 in the ancestral sea turtle lineage, followed by an expansion in the green turtle but a further contraction in  
200 the leatherback turtle. Similar trends were detected for OR Class II genes, but with a greater magnitude of  
201 contraction in the ancestral sea turtle lineage followed by a further contraction for the leatherback turtle  
202 and only a small expansion for the green turtle.

203 A second important RRC encompassed the major histocompatibility complex (MHC), which  
204 plays a critical role in vertebrate immunity and has particularly strong relevance to sea turtle conservation  
205 due to the threat of FP and other diseases (32). In addition to the MHC genes, this RRC (RRC14) includes  
206 several copies of OR Class II genes, zinc-finger protein genes and other genes involved with immunity,  
207 such as butyrophilin subfamily members and killer cell lectin-like receptors (Fig. 2d, Table S12).  
208 Invariably, the green turtle carried higher numbers of all the multicopy genes present in RRC14. RRCs on  
209 other chromosomes also showed increased levels of zinc-finger protein genes in the green turtle,  
210 including the RRCs labeled 6A, 11A, 14A, and 28 (Table S3). In particular, zinc-finger protein genes  
211 were highly prevalent on chromosomes 14 and 28 in both sea turtles, representing more than 50% of all  
212 the protein domains present on these chromosomes (Fig. S8).

213 Finally, given the critical importance of understanding the underlying mechanism of temperature-  
214 dependent sex determination (TSD) in the face of climate change, we analyzed genes known to be

215 associated with TSD across reptiles. Almost all 216 genes previously implicated in male- or female-  
216 producing pathways in reptilian species with TSD were single-copy genes in both sea turtle species  
217 (Table S7; 210 genes per species). Only three genes (*MAP3K3*, *EP300*, and *HSPA8*) were duplicated in  
218 both genomes, with the copies located on different chromosomes in all cases. Moreover, homologous  
219 genes were generally located in the same region of the genomes for both species (Fig. S9), and missing  
220 genes were typically absent in both species, with only four genes found in one species but not the other  
221 (Table S7).

222

### 223 *Macro and microchromosomes*

224 Microchromosomes contained higher proportions of genes than macrochromosomes (Fig. 3a,b),  
225 and gene content was strongly positively correlated with GC content (Fig. S10). These patterns were  
226 particularly apparent in small (<20 Mb) microchromosomes, where GC content reached 50%, compared  
227 to the 43 - 44% genome-wide averages. Within chromosome groups, larger proportions of multicopy  
228 genes were generally associated with higher total gene counts, and chromosomes with the highest  
229 multicopy genes numbers have increased proportions of RRCs (Fig. 3a,b).

230 Mean genetic distances for single-copy regions between the two sea turtles were also higher in  
231 small microchromosomes (0.053) compared to both intermediate (>20 Mb) microchromosomes (0.047),  
232 and macrochromosomes (0.045) (Fig. 3c). However, examination of intermediate microchromosome and  
233 macrochromosome RRCs revealed elevated genetic distances in these regions that approached values  
234 observed in small microchromosomes (Table S8). Genetic distances were also positively correlated with  
235 heterozygosity, which was higher in small microchromosomes for both species (Figs. 3d & S11-13).

236

### 237 *Genome diversity*

238 Although both species displayed similar patterns of higher heterozygosity in microchromosomes  
239 than macrochromosomes (Figs. 3d & S11-13), they differed in the genome-wide nucleotide diversity level  
240 by almost an order of magnitude (repeat masked  $\pi = 3.19 \times 10^{-4}$  leatherback and  $22.2 \times 10^{-4}$  green turtle;  
241 Fig. S12, Table S9). Exonic regions exhibited lower levels of heterozygosity than non-coding regions  
242 (Fig. 4a, Table S9), with a greater reduction in heterozygosity within green turtle exons (~20%) than  
243 leatherback turtle exons (~10%) compared to genome-wide levels. In addition, the percentage of 100 Kb  
244 windows containing zero heterozygous sites was higher in the green turtle (6.60%) than the leatherback  
245 turtle (2.87%), suggesting that although diversity was lower overall in the leatherback turtle, it was more  
246 evenly spread across the genome than in the green turtle. Using a standardized heterozygosity pipeline  
247 (see Methods; Fig. 4b), we found the genomic diversity of the leatherback turtle was substantially lower  
248 than almost all other reptiles examined, including *Chelonoidis abingdonii*, where low diversity has been  
249 considered a contributing factor to their extinction (53), and only the critically endangered Chinese  
250 alligator (*Alligator sinensis*) showed lower diversity (54). In contrast, the genomic diversity of the green  
251 turtle fell in the mid-range for reptiles, as well as similar analyses conducted on mammals (55, 56).  
252 Finally, we identified high-diversity exonic regions using multiple approaches (see Methods), and found  
253 that many contained immune, OR, and zinc-finger protein genes in both species, but especially for the  
254 green turtle which showed a greater number of high-diversity windows (Fig 4c; Table S10). Given the  
255 striking similarity to the RRC analysis results above, these findings independently reinforced the  
256 importance of these gene families in the divergent evolution of these species.

257

258 *Runs of homozygosity (ROH)*

259 The leatherback turtle had a greater number of ROHs (>100 Kb) compared to the green turtle  
260 ( $N_{\text{ROH}} = 2,045$  and 873, respectively), as well as higher accumulated length and proportion of the genome  
261 in ROH ( $S_{\text{ROH}} = 400.61$  Mb (18.51% of genome) and 327.06 Mb (15.53%), respectively). The average  
262 length of ROHs was generally shorter in the leatherback turtle ( $L_{\text{ROH}} = 196$  Kb and 375 Kb for the  
263 leatherback and green turtles, respectively; Fig. 4d), with the accumulated length of short (<500 Kb)  
264 ROHs highest when compared to medium (500 Kb-1 Mb) and long ROHs (>1 Mb) (Fig. 4d). The  
265 leatherback turtle genome only showed one ROH that was greater than 1 Mb in length, suggesting that  
266 recent bottlenecks or inbreeding are unlikely, rather that this species has maintained long-term low  
267 diversity. In contrast, the green turtle had 54 ROHs longer than 1 Mb, suggestive of a possible more  
268 recent population bottleneck or inbreeding events. The average lengths of ROHs were also higher in  
269 macrochromosomes than microchromosomes (Fig. S15).

270

271 *Genetic load*

272 Coding region variants of the leatherback turtle genome were found more likely to be impactful,  
273 with 0.10% and 0.07% of variants predicted to cause ‘high impacts’ (e.g., stop-codon gain or loss) for the  
274 leatherback and green turtles, respectively, and with ‘moderately’ and ‘low’ impact variants also higher in  
275 the leatherback turtle (Fig. 4e). Additionally, the missense to silent mutation ratio was higher in the  
276 leatherback (0.89) than green turtle (0.65), again indicating that genetic load is higher for the leatherback  
277 turtle. High-impact variants predicted by snpEff only occurred in one species for any given gene. The 103  
278 and 357 nucleotide variants characterized as ‘high’ impact in the leatherback and green turtle were found  
279 within 59 and 171 unique genes, respectively. The functions of these genes were variable (Fig. S16). For  
280 the leatherback turtle, many of the genes impacted were linked to cell transport and demethylation, with  
281 DEAH-box helicase 40 and a *Hsp40* family member also impacted (Table S13). In contrast, for the green  
282 turtle, many of the genes were linked to immunity, including an MHC class I alpha chain gene, as well as  
283 B-cell receptors and killer-cell receptors. The green turtle also showed putative high impact variants  
284 within several OR genes.

285

286 *Demographic history*

287 Pairwise Sequential Markovian Coalescence (PSMC) analyses indicated different historical  
288 effective population sizes ( $N_e$ ) between the two sea turtle species (Fig. 4f). The results indicate that the  $N_e$   
289 for the leatherback turtle has been relatively small and sustained, ranging in size from approximately  
290 2,000 to 21,000 over the last 10 million years, and at the lower end of this range for the last 5 million  
291 years. In comparison, the green turtle has experienced wider population fluctuations and a relatively  
292 higher overall  $N_e$  suggesting that  $N_e$  has fluctuated between approximately 44,000 and 83,000. While the  
293  $N_e$  for the leatherback turtle is relatively low, it showed signs of increasing abundance prior to the Eemian  
294 warming period (Fig. 4f [H]), with a subsequent decrease during this period until the last glacial  
295 maximum (LGM). In contrast, the green turtle had three distinct peaks in  $N_e$  (Fig. 4f), potentially  
296 associated with ocean connectivity changes related to the closure of the Tethys Sea [A], the Pleistocene  
297 period [B], and a more pronounced peak that aligns with later marked temperature fluctuations [C]. We  
298 observed similar patterns for PSMC analyses conducted on additional individuals for both species (see  
299 Supplementary Appendix I).

300

301 **Discussion**

302

303 ***Divergence in localized RRCs and microchromosomes amidst high global genome synteny.*** The  
304 lineages leading to leatherback and green turtles diverged over 60 MYA (4), giving rise to species that are  
305 adapted to dissimilar habitats, diets, and modes of life. Despite high overall levels of genome synteny  
306 across both the macro- and microchromosomes between the sea turtle families, RRCs and small  
307 microchromosomes were particularly associated with high concentrations of multicopy gene families, as  
308 well as heightened genomic diversity and genetic distances between species, suggesting that these  
309 genomic elements may be important sources of variation underlying phenotypic differentiation. Though  
310 our results here do not demonstrate direct causality, we have identified candidate regions and gene  
311 families that can be targeted in further studies quantifying evidence for positive selection and their roles  
312 in sea turtle adaptation and speciation.

313 The high global stability of both macro- and microchromosomes between sea turtle families also  
314 aligns with recent work showing similar patterns across reptiles including birds, emphasizing the  
315 important roles of microchromosomes in vertebrate evolution (57). However, it is not yet clear if the  
316 characteristics of microchromosomes and RRCs we observed are unique to sea turtles, or, more likely,  
317 commonly observed in other vertebrates. Our detailed analyses of RRCs, microchromosomes, and their  
318 associated genes were only possible due to the high-quality of the assembled sea turtle genomes because  
319 these analyses can be sensitive to genome fragmentation and misassemblies (39). The prevalence or  
320 importance of such localized genomic differentiation among other closely or more distantly related  
321 reptiles or other vertebrate groups has not been evaluated due to a lack of equivalent genomic resources,  
322 but this is rapidly changing. As chromosomal-level genomes across all vertebrate lineages soon become  
323 available, our work provides a roadmap for identifying genomic regions harboring contrasting  
324 expansion/contractions of gene families and diversity levels in different vertebrate lineages. For taxa with  
325 highly conserved genomes like sea turtles, analyses of RRCs and microchromosomes are likely important  
326 to understand their divergent evolutionary histories and the phenotypic connections of the genes within  
327 them.

328

329 ***Contrasting sensory and immune gene evolution between sea turtle families.*** Sea turtles have complex  
330 sensory systems and can detect both volatile and water-soluble odorants, which are imperative for  
331 migration, reproduction and identification of prey, conspecifics, and predators (58–62). However,  
332 leatherback and green turtles occupy dissimilar ecological niches that depend on different sensory cues.  
333 While leatherback turtles inhabit the pelagic environment their entire lives post-hatching, performing  
334 large horizontal and vertical migrations to seek out prey patches of jellyfish and ctenophores (63), green  
335 turtles recruit as juveniles to neritic coastal and estuarine habitats and can have highly variable diets (64,  
336 65). Substantial differences have been detected in the morphology of sea turtle nasal cavities, with  
337 leatherback turtle cavities relatively shorter, wider, and more voluminous than chelonids (66–68),  
338 suggesting reduced requirements for olfactory reception. OR genes encode proteins used to detect  
339 chemical cues, with the number of OR genes present in a species' genome strongly correlated to the  
340 number of odorants that it can detect (69), and linked to the chemical complexity of its environment (70).  
341 The two major groups of ORs in amniote vertebrates are separated by their affinities with hydrophilic  
342 molecules (Class I) or hydrophobic molecules (Class II) (71). Class I OR genes may be particularly  
343 important in aquatic adaptation (32), and expansions of Class I ORs in testudines, including green turtles,  
344 have been previously reported, although with some uncertainty due to the use of short-read assemblies



345 (32, 41, 72). Our reconstruction of both Class I and Class II OR gene evolution throughout the sea turtle  
346 lineage revealed that after ancestral contractions, gene copy evolution diverged in opposite directions  
347 between the sea turtle families. The greater loss of Class II compared to Class I ORs in the ancestral sea  
348 turtle lineage likely reflects relaxed selection for detection of airborne odorants, as has been observed in  
349 other lineages that recolonized marine environments, including marine mammals (73). However, as sea  
350 turtles continue to use terrestrial habitats for reproduction, they need to retain some of these capabilities,  
351 which could explain why the contraction was weaker than observed in fully marine species (e.g., the  
352 vaquita *Phocaena sinus*; Fig. 2e).

353 The strong Class I OR expansion in the green turtle may be related to its distribution in complex  
354 neritic habitats and variable diet, requiring detection of a high diversity of waterborne odorants, while the  
355 continued loss of ORs in the leatherback turtle could be a consequence of its more specialized diet and  
356 lower complexity of pelagic habitats. Although leatherback turtles can detect jellyfish chemical cues,  
357 sensory experiments have indicated that visual cues are more important for food recognition in this  
358 species (74). Additionally, while the precise mechanisms underpinning philopatry in sea turtles still  
359 remain unclear, green turtles are thought to use olfactory cues to reach natal nesting beaches following  
360 long-distance navigation guided by magnetoreception (60, 62). Leatherback turtles exhibit more  
361 'straying' from natal rookeries than other species, and such relaxed philopatry may be related to reduced  
362 capabilities or reliance on olfactory cues to hone in on specific beaches.

363 The diversity of the highly-complex MHC region is a key component in the vertebrate immune  
364 response to novel pathogens, with greater gene copy numbers and heterozygosity linked to lower disease  
365 susceptibility (75). While both sea turtle species contained most of the core MHC-related genes, the green  
366 turtle had more copies of genes involved in adaptive as well as innate immunity. Pathogen prevalence and  
367 persistence is often greater in neritic habitats than open ocean habitats (76), so green turtles may be  
368 exposed to higher pathogen loads and diversity than leatherback turtles (77). However, reptilian immune  
369 systems are understudied compared to other vertebrates, and very few studies of MHC genes have been  
370 conducted in turtles (78). Thus, it is not yet understood how immune gene diversity translates into disease  
371 susceptibility or ecological adaptation in sea turtles, which is particularly critical for their conservation as  
372 FP continues to threaten the recovery of populations around the globe (30). Although this viral-mediated  
373 tumor disease occurs in all sea turtle species, there is high variation between species and populations in  
374 disease prevalence and recovery, making it plausible that harboring certain genes, copy numbers, or  
375 specific alleles may play important roles in disease dynamics. Despite decades of research there have  
376 been no studies of the immunogenomic factors governing FP susceptibility or resilience, in part due to  
377 difficulty in accurately quantifying hypervariable and complex MHC loci with short-read sequencing  
378 technologies (79). Our reference genomes now enable studies accurately interrogating MHC and other  
379 immune loci to close this critical research gap, and advance our fundamental understanding of immune  
380 gene evolution in sea turtles.

381  
382 ***Conservation of reproductive genes and repetitive elements.*** In contrast to olfactory and immune genes,  
383 almost all genes with *a priori* linkages to TSD pathways (80–82) occurred as single copy orthologs with  
384 highly conserved chromosomal locations between the two species. This is likely indicative of strong  
385 selection for conservation of this reproductive pathway, but our understanding of the specific roles these  
386 genes play in sea turtle TSD remains limited. Resolving whether inter- (83) and intra-specific (84)  
387 variations in thermal thresholds are due to the few genes that diverged from the general pattern we  
388 observed, functional sequence variation between orthologs, or other factors (e.g., epigenetic processes) is

389 of high conservation concern for sea turtles (85), as climate warming is expected to skew sex ratios and  
390 alter population demographics (86) in the absence of substantial plasticity or adaptation. Our results serve  
391 as the foundation for these much-needed studies to quantify genomic mechanisms of TSD in sea turtles  
392 and determine their adaptive capacity to persist under climate change.

393 While REs in turtles have been investigated for over 30 years (87, 88), few studies have directly  
394 addressed the distribution and diversity of REs within testudine genomes (89). Both sea turtle genomes  
395 have substantially larger RE compositions (>40%) than previous estimates for other turtle species (41, 89,  
396 90), including the draft genome of the green turtle (10% of the genome (41)). Interestingly, more recent  
397 reptile genome assemblies show higher proportions of REs (90, 91), with results similar to our estimates.  
398 The benefits of whole-genome approaches are further highlighted in the tuatara, where initial RE  
399 estimates suggested <10% of the genome was composed of REs (92), yet a subsequent whole-genome  
400 assembly increased this estimate to 64% (45). Collectively, these results support the notion that RE  
401 patterns could be more conserved across non-avian reptiles than previously believed, and the continued  
402 application of recent advances in genome sequencing, assembly methods, and analyses are needed to  
403 better understand the RE patterns and the processes that generate them (39, 43).

404  
405 ***Differential genomic diversity and demographic histories.*** Genomic diversity is a critical metric for  
406 evaluating extinction risk and adaptive potential to environmental perturbation (93–95), with  
407 heterozygosity positively correlated with individual fitness (see reviews by (96, 97). Understanding the  
408 causes and consequences of genomic diversity is imperative for sea turtles, and for leatherback turtles in  
409 particular, where contemporary populations have experienced recent sharp declines due to human  
410 activities (25). The leatherback turtle genome exhibited exceptionally low diversity relative to the green  
411 turtle, other reptiles and mammals, broadly aligning with previous estimates (98, 99). However, factors  
412 influencing genomic diversity can vary among species (100), and our PSMC and ROH results indicate  
413 that low diversity in the leatherback turtle is likely a consequence of long-term low effective population  
414 sizes rather than recent population reductions. This is consistent with mitochondrial analyses suggesting  
415 that contemporary populations radiated from a small number of matriarchal lineages within a single  
416 refugium following the Pleistocene (99). The low, relatively evenly spread heterozygosity is also  
417 congruent with sustained low population sizes with frequent outbreeding similar to that observed in  
418 several mammal species (101, 102). Also encouragingly, although the reference genome was generated  
419 from an individual from the West Pacific leatherback turtle population that has suffered precipitous  
420 declines (103), we did not detect patterns consistent with recent inbreeding. This suggests that if ongoing  
421 anthropogenic threats are mitigated, the population may still be large enough to avoid complications  
422 arising through inbreeding depression during recovery. However, the possibility that population declines  
423 have occurred too rapidly for the impacts of inbreeding to yet be detected warrants cautious optimism and  
424 the need for continued genomic monitoring of the population. In contrast, the higher genomic diversity  
425 with some long ROHs observed in the green turtle likely reflects their radiation from many refugia (104),  
426 as well as relatively recent inbreeding events. This is potentially because the green turtle genome was  
427 generated from an individual from the Mediterranean population where nesting populations are relatively  
428 small (105) which, combined with strong natal philopatry (106), may increase the chance of inbreeding.

429 Regardless of the causes of current genomic diversity levels in sea turtles, the amount of standing  
430 variation may have important implications for their future persistence (107), especially given the adaptive  
431 capacity likely required to keep pace with rapid anthropogenic global change. With extremely low  
432 genomic diversity and a higher genetic load compared to the green turtle, the risks are presumably of

433 greater concern for leatherback turtles. Additionally, leatherback turtles have substantially lower hatching  
434 success compared to other sea turtle species (29) that is potentially related to the heightened genetic load  
435 and low heterozygosity (108, 109), and may combine with other factors to slow population recoveries  
436 following conservation measures. However, recent studies have documented low genome diversity in a  
437 number of species with wide geographic distributions and relatively large census population sizes,  
438 including some long-lived marine vertebrates (101, 110–113). Other species with low diversity have  
439 rebounded following population declines and/or appear to have purged deleterious alleles through long-  
440 term low population sizes (111, 114, 115), thereby limiting the impact of low genomic diversity on  
441 viability (56, 111, 116). Although our results of a greater genetic load despite long-term low  $N_e$  suggest  
442 this is not the scenario for leatherback turtles, further assessments of more individuals over greater spatial  
443 and temporal are needed. Studies enabled by the reference genomes presented here quantifying diversity  
444 and genetic load within and among global populations will clarify these relationships for leatherback  
445 turtles and other sea turtle species to guide conservation recommendations.

446 In contrast to the long-term low  $N_e$  of leatherback turtles, our demographic reconstructions  
447 showed the  $N_e$  of the green turtle has fluctuated widely over the same period. These fluctuations appear  
448 correlated with climatic events, beginning with the closure of the Tethys Sea, which altered ocean  
449 connectivity and represented a period of increasing temperatures that may have opened more suitable  
450 habitat. As temperatures subsequently decreased,  $N_e$  also decreased, however temperature fluctuations  
451 during the Pleistocene were associated with an additional increase in  $N_e$ , and a subsequent increase in  $N_e$   
452 was associated with warmer temperatures following the Eemian period. While warmer temperatures  
453 presumably allowed for larger population sizes of green turtles, spikes in  $N_e$  (e.g., ~100KYA) are most  
454 likely associated with mixing of previously isolated populations due to warm-water corridors allowing  
455 movement between populations and ocean basins (117). The lower, long-term  $N_e$  of leatherback turtles  
456 may reflect a reduced census size associated with this species' greater mass and trophic position.  
457 Following an initial decrease in  $N_e$  associated with declining temperatures, the  $N_e$  of leatherback turtles  
458 remained relatively constant throughout the fluctuations of the Pleistocene. Although reptiles are  
459 generally sensitive to climatic thermal fluctuations, leatherback turtles exhibit unique physiological  
460 adaptations that produce regional endothermy and facilitate exploitation of cold-water habitats (6) that  
461 potentially led them to being less susceptible to periods of cooler temperatures. While our overall  
462 estimates and trends for both species were broadly concordant with previous studies (99, 118, 119), a  
463 recent study using MSMC found steep declines in  $N_e$  for green turtles >100,000 years before present  
464 (119), which was not detected in our PSMC analyses. Since this decline was also not detected in a prior  
465 study using PSMC on the draft the green turtle genome (118), this is likely a consequence of the different  
466 methods, with MSMC analyses inferring large  $N_e$  for more ancient time scales (120).

467  
468

469 ***Enabling future research and conservation applications.*** In addition to the insights reported here, the  
470 reference genomes for both extant sea turtle families provide invaluable resources to enable a wide  
471 breadth of previously unattainable fundamental and applied research. Combined with other forthcoming  
472 chromosomal-level vertebrate genomes, in-depth comparative genomics analyses can further investigate  
473 ecological adaptation related to immune and sensory gene evolution, as well as the genomic basis for  
474 traits of interest such as adaptation to saltwater, diving capacity, and long-distance natal homing. Studies  
475 leveraging these reference genomes alongside whole-genome sequencing of archival sample collections  
476 can assess how genomic erosion, inbreeding and mutational load are linked to population size,

477 trajectories, and conservation measures in global sea turtle populations. For instance, the fact that  
478 leatherback turtles have persisted with low diversity and  $N_e$  for long time periods offers hope for their  
479 recovery, but given that some populations have now been reduced to only a few hundred individuals  
480 (103), research quantifying purging of deleterious alleles, inbreeding depression and adaptive capacity  
481 within populations is urgently needed (121). Many conservation applications that may not require whole-  
482 genome data can also benefit from the utility of these reference genomes, including the development of  
483 amplicon panels and molecular assays to investigate TSD mechanisms and adaptive capacity under  
484 climate change, and assessing linkages between immune genes and disease risk. Finally, with global  
485 distributions and long-distance migratory connectivity, sea turtle conservation requires international  
486 collaboration that has been previously hampered by difficulty comparing datasets between laboratories.  
487 Existing anonymous markers can now be anchored to these genomes, and new ones can be optimized for  
488 conservation-focused questions and shared across the global research community, facilitating large-scale  
489 syntheses and equitable capacity building for genomics research. While ongoing anthropogenic impacts  
490 continue to threaten the viability of sea turtles to persist over the coming century, combined with the  
491 important work of reducing major threats such as fisheries bycatch and habitat loss, these genomes will  
492 enable research that make critical contributions to recovering imperiled populations.

493

## 494 **Methods**

### 495 *Sample collection, genome assembly and annotation*

496 Blood was collected from leatherback and green turtles using minimally invasive techniques for  
497 isolation of ultra-high molecular weight DNA, and tissue samples of internal organs for RNA were  
498 collected opportunistically from recently deceased or euthanized animals. Full details of sample  
499 collection, storage, and laboratory processing prior to sequencing can be found in Supplementary  
500 Appendix I. Resulting raw data were deposited into the VGP Genome Ark and NCBI Short-Read Archive  
501 (SRA) (see Data Accessibility Statement). We assembled both genomes using four genomic technologies  
502 following the VGP pipeline v1.6 (39) with a few modifications detailed in Supplementary Appendix I.  
503 Briefly, PacBio Continuous Long Reads were assembled into haplotype phased contigs, with contigs  
504 scaffolded into chromosome-level super scaffolds using a combination of 10X Genomics linked reads,  
505 Bionano Genomics optical maps, and Arima Genomics Hi-C 3D chromosomal interaction linked reads.  
506 Base call errors were corrected to achieve high quality ( $>Q40$ ). The assemblies were manually curated,  
507 with structural errors corrected according to the Hi-C maps (Fig. S1), and the 28 super scaffolds  
508 (hereinafter referred to as chromosomes) numbered in both species according to sequence lengths in the  
509 leatherback turtle assembly, and synteny between the two species. A manual inspection comparing the  
510 sequence collinearity between the first curated versions of the genomes revealed a small number of  
511 artefactual sequence rearrangements that were corrected in a second round of manual curation (see  
512 Supplementary Appendix D).

513 To enable accurate, species-specific annotations for each genome, both short and long-read  
514 transcriptomic data (RNA-Seq and Iso-Seq) were generated from tissues known for their high transcript  
515 diversity in each species. These data, plus homology-based mapping from other species, were used to  
516 annotate the genomes using the standardized NCBI pipeline (122). Briefly, we performed annotation as  
517 previously described (39, 123), using the same RNA-Seq, Iso-Seq, and protein input evidence for the  
518 prediction of genes in the leatherback and green turtles. We aligned 3.5 billion RNA-Seq reads from eight  
519 green turtle tissues (blood, brain, gonads, heart, kidney, lung, spleen and thymus) and 427 million reads  
520 from four leatherback turtle tissues (blood, brain, lung and ovary) to both genomes, in addition to 144,000

521 leatherback turtle and 1.9 million green turtle PacBio IsoSeq reads, and all Sauropsida and *Xenopus*  
522 GenBank proteins, known RefSeq Sauropsida, *Xenopus*, and human RefSeq proteins, and RefSeq model  
523 proteins for *Gopherus evgoodei* and *Mauremys reevesii*.

524

#### 525 *Genome quality analysis*

526 We used the pipeline assembly-stats from <https://github.com/sanger-pathogens/assembly-stats> to  
527 estimate the scaffolds N50, size distributions and assembly size. BUSCO analysis (115) and QV value  
528 estimations (116) were conducted to assess the overall completion, duplication, and relative quality of the  
529 assemblies. We used D-GENIES (118) with default parameters to conduct dot plot mapping of the entire  
530 genomes and each individual chromosomes to evaluate the synteny between leatherback and green turtle  
531 genomes, and Haibao Tang JCVI utility libraries following the MCScan pipeline (119) to verify the  
532 contiguity of the genomes. Incongruences in gene synteny blocks were manually investigated using  
533 Artemis Comparative Tool (120), identifying possible regions of inversion that could be caused by  
534 artifacts during assembly. These regions were then identified and corrected in the latest version of the  
535 assembly for both species. Only a few structural rearrangements between the two species remained after  
536 two rounds of manual curation with support of sequencing data. The final curated assemblies were  
537 analyzed using the Genome Evaluation Pipeline (<https://git.imp.fu-berlin.de/cmazzoni/GEP>) to obtain all  
538 final QC plots and summary statistics.

539

#### 540 *Identification and analysis of RRCs and REs*

541 Leatherback and green turtle genomes were mapped to each other using Minimap2 with a dot plot  
542 of the mapping generated using D-GENIES (124). Using windows of 20 Mb, the dot plot was screened  
543 visually with regions larger than 1 Mb showing reduced collinearity (i.e., one or more breaks in the  
544 diagonal indicating homology), as well as smaller regions with obvious signals of genomic  
545 rearrangements (e.g., inversions), cataloged as regions of reduced collinearity (RRCs). Several genomic  
546 features were examined within these regions and compared to regions of the same length directly up- and  
547 down-stream of the RRCs (Table S3). We identified the functions of the genes present in RRCs using  
548 genome annotations and identified protein domains using Interproscan (125). The proportion of GO terms  
549 in each chromosome was estimated for each species using PANTHER (126); Fig. S16). To examine if  
550 RRCs presented differential patterns of sequence and/or gene duplication between the species, we aligned  
551 the genomes of the sea turtles against each other using Progressive Cactus (127, 128), and all homologous  
552 genes that presented more than one copy for one of the two species were isolated using an inhouse script  
553 (*IdentifyDupsReciprocalBlast.sh*) to retrieve duplicated genes (see Supplementary Appendix I for further  
554 details on Cactus alignments). Repetitive elements (REs) were identified by creating a *de novo* database  
555 of transposable elements using RepeatModeller2 (129), followed by running RepeatMasker (130, 131) to  
556 calculate Kimura values for all REs (see full analysis details in Supplementary Appendix I).

557

#### 558 *Gene families and gene functional analysis*

559 To estimate the timing of gene family evolution for the OR gene families on sea turtles we used  
560 Computational Analysis of gene Family Evolution v5 (132). Briefly, CAFE5 uses phylogenomics and  
561 gene family sizes to identify gene family expansions and contractions, we used a dataset containing 8  
562 species of turtle, 4 non-turtle reptiles, 3 mammals and 1 amphibian using OrthoFinder (133, 134). OR  
563 orthogroups were grouped based on subfamily (Class I and Class II; see (72)), and an ultrametric

564 phylogeny was generated by gathering 1:1 orthologs. We then aligned amino acid sequences for each  
565 orthogroup and generated a phylogenetic tree (see Supplementary Appendix I for details).

566 Like many reptile species, sea turtles possess TSD. We compiled a list of 217 genes that have  
567 been implicated in TSD in reptiles (see Table S7). To determine if these genes were present in our  
568 assembled genomes, we employed two methods of investigation. We firstly searched the genome  
569 annotations for gene identifiers and protein names, followed by a BLAST search of homologous  
570 sequences to account for variations in gene identifiers between taxonomic groups (see Supplementary  
571 Appendix I for details). Resultant locations on both genomes were plotted on a Circos plot CIRCA  
572 (<http://omgenomics.com/circa>).

573 To identify genes related to immunity, and the MHC in particular, we searched the genome for  
574 the list of core MHC genes provided in Gemmell et al. (2020) (45). Genes were searched for in a similar  
575 way to the method used for the TSD genes, with initial searches of gene identifications, followed by a  
576 search of protein identifiers. As genes associated with the MHC are diverse, and vary substantially among  
577 species, we did not use a BLAST search for these genes. Locations of the genes were then compared  
578 between species to determine which genes were annotated, and where the core MHC region is located  
579 within the genomes.

580

#### 581 *Genetic distance, genome diversity, runs of homozygosity, and historical demography*

582 In order to estimate the genetic distance between the leatherback and green turtle genomes, we  
583 used the halSnps pipeline (135) to compute interspecific single variants based on genome alignments  
584 obtained with Progressive Cactus (127, 128) using the leatherback turtle genome as the reference. Genetic  
585 distances were calculated for windows across the genome where each window included exactly 10,000  
586 positions presenting single alignments against the green turtle genome in the Cactus output. Positions  
587 with zero, or more than one alignment were ignored, and if this occurred over more than 50% of a given  
588 window, it was skipped entirely (i.e., each window analyzed covered between 10 and 20 Kb of the  
589 genome). Interspecific distances per bp were calculated by dividing the number of variants found within a  
590 window by 10,000.

591 We calculated genome-wide heterozygosity using a method adapted from Robinson et al. (2019)  
592 (102). Briefly, we used the Genome Analysis Toolkit (GATK) (136) to call genotypes at every site across  
593 the genome using the 10X reads sourced from the reference individual mapped back to the reference  
594 genomes using BWA-mem (137). Heterozygosity was calculated within 100 Kb non-overlapping  
595 windows, with only sites that had a depth of between  $\frac{1}{3}\times$  and  $2\times$  mean coverage retained for genotype  
596 scoring. Heterozygosity was calculated within these windows for (1) the entire genome, (2) the genome  
597 with repeat-regions masked, (3) only exon regions, (4) and for regions that were classified as ‘non-exons.’  
598 We also adapted this pipeline to generate genome-wide heterozygosity for a number of additional  
599 reptilian and outgroup species with sequences sourced from the NCBI SRA where species-specific  
600 reference genomes were available (see details in Supplementary Appendix I).

601 ROHs were calculated by initially generating an additional SNP-list using whole-genome re-  
602 sequenced information from five additional individuals for each species (Table S11). This SNP-list was  
603 generated through the Analysis of Next Generation Sequencing Data (ANGSD; (138) pipeline due to the  
604 low- to moderate-coverage of the additional samples ( $\sim 2$ - $13\times$ ). ANGSD was parameterized to output files  
605 that were configured for use as input for the ROH analysis incorporated in PLINK (139). ROHs were then  
606 further characterized as ‘short’ (100-500 Kb), ‘medium’ (500Kb-1 Mb), or ‘long’ ( $>1$  Mb) based on their  
607 length. ROHs for only the reference individuals are presented.

608 The alignments of the 10X reads for the reference individuals were also used as input for Pairwise  
609 Sequential Markovian Coalescence (PSMC; (140)) analysis of demographic history for both species. We  
610 used SAMtools (141) and BCFtools (142) to call genotypes with base and mapping quality filters of  
611  $>Q30$ . We also filtered for insert size (50-5,000bp) and allele balance (AB) by retaining only biallelic  
612 sites with an AB of  $<0.25$  and  $>0.75$ . We then ran PSMC analysis using the first 10 scaffolds, which  
613 constituted over 84% of the total length of the genome, using a generation time of 30 years (mid-way  
614 between reported generation times for both species; see Supplementary Appendix I), and a mutation rate  
615 of  $1.2 \times 10^{-8}$  (118).

#### 616 617 *Genetic load*

618 Estimates of deleterious allele accumulation were conducted using the snpEff variant annotation  
619 software (143). We estimated the impacts of variants from coding regions using the species-specific  
620 genome annotations generated for both species, with a total of 18,775 genes for the leatherback turtle  
621 genome, and 19,752 genes for the green turtle genome used in the analysis. Variants were only included  
622 in the analyses if they met stringent quality requirements, with loci filtered during genotyping based on  
623 depth of coverage ( $\frac{1}{3} \times - 2 \times$  mean coverage) and base quality metrics ( $Q < 20$ ). The snpEff program  
624 predicts variant impacts and bins them into 'high', 'moderate', or 'low' impact categories, and outputs a  
625 list of genes that have predicted variant effects.

#### 626 627 **Acknowledgments**

628 We are grateful for the assistance with the (1) leatherback turtle sample collection from the St. Croix Sea  
629 Turtle Program and the US Fish and Wildlife Service, the NOAA-SWFSC California in-water leatherback  
630 research team, and the New England Aquarium; (2) green turtle sample collection from the Israel  
631 National Sea Turtle Rescue Centre, the NOAA PIFSC-MTBAP team, and Thierry Work (USGS). We  
632 also thank Estefany Argueta and Jamie Stoll for assistance with literature searches for TSD and immune  
633 genes, and Phillip Morin, Andrew Foote, Anna Brüniche-Olsen, Annabel Beichman, Morgan McCarthy,  
634 David L. Adelson, and Yuanyuan Cheng for their invaluable discussions surrounding analysis approaches  
635 and comments on the manuscript. Sequencing of the green turtle has been performed by the Long Read  
636 Team of the DRESDEN-concept Genome Center, DFG NGS Competence Center, part of the Center for  
637 Molecular and Cellular Bioengineering (CMCB), Technische Universität Dresden and MPI-CBG.

#### 638 639 **Funding**

640 Funding was provided by the University of Massachusetts Amherst, NSF-IOS (grant #1904439 to LMK),  
641 NOAA-Fisheries, Vertebrate Genomes Project, Rockefeller University, to EDJ, HHMI to EDJ, the Sanger  
642 Institute, Max-Planck-Gesellschaft, as well as grant contributions from Tom Gilbert, Paul Flicek, Robert  
643 Murphy, Karen A. Bjørndal, Alan B. Bolten, Ed Braun, Neil Gemmell, Tomas Marques-Bonet, and Alan  
644 Scott. We also acknowledge CONICYT-DAAD for scholarship support to TCV, and EKSR was  
645 supported by São Paulo Research Foundation - FAPESP (grant #2020/10372-6). BeGenDiv is partially  
646 funded by the German Federal Ministry of Education and Research (BMBF, Förderkennzeichen  
647 033W034A). The work of FT-N and PM was supported by the Intramural Research Program of the  
648 National Library of Medicine, National Institutes of Health. The work of MP was partially funded  
649 through the Federal Ministry of Education and Research (grant 01IS18026C). HP was supported by a  
650 Formació de Personal Investigador fellowship from Generalitat de Catalunya (FI\_B100131). MK was

651 supported by “la Caixa” Foundation (ID 100010434), fellowship code LCF/BQ/PR19/11700002 and the  
652 Vienna Science and Technology Fund (WWTF) and the City of Vienna through project VRG20-001.

653

#### 654 **Data Accessibility Statement**

655 Assemblies for both species have been deposited on NCBI GenBank. The NCBI GenBank accession  
656 numbers for the leatherback turtle genome assembly (rDerCor1) are GCF\_009764565.3 and  
657 GCA\_009762595.2 for the annotated primary and original alternate haplotypes in BioProject  
658 PRJNA561993, and for the green turtle assembly (rCheMyd1) are GCF\_015237465.2 and  
659 GCA\_015220195.2 for primary and alternate haplotypes respectively in BioProject PRJNA561941. The  
660 raw data used for assemblies are available on the Vertebrate Genome Ark

661 (<https://vgp.github.io/genomeark/>). The leatherback turtle RNA-Seq data generated for the purpose of  
662 assembly annotation was deposited in the SRA under accession numbers SRX8787564-SRX8787566  
663 (RNA-Seq) and SRX6360706-SRX6360708 (ISO-Seq). Green turtle RNA-Seq data generated for  
664 annotation were deposited in SRA under accessions SRX10863130-SRX10863133 (RNA-Seq) and as  
665 SRX11164043-SRX11164046 (ISO-Seq). All scripts used for downstream analyses following genome  
666 assembly and annotation have been deposited on GitHub under repository

667 [https://github.com/bpbentley/sea\\_turtle\\_genomes](https://github.com/bpbentley/sea_turtle_genomes).



668 **Tables and Figures**

669  
670 **Table 1** | Quality statistics for the genome assemblies and annotations for leatherback (*Dermochelys coriacea*) and green (*Chelonia mydas*)  
671 turtles.

	Leatherback turtle ( <i>Dermochelys coriacea</i> )	Green turtle ( <i>Chelonia mydas</i> )
Genome ID	rDerCor1	rCheMyd1
Assembly accession	GCA_009764565.3	GCA_015237465.1
Assembly level	Chromosome	Chromosome
Total genome length	2,164,762,090 bp	2,134,358,617 bp
Contig N50	7,029,801	39,415,510
Scaffold N50	137,568,771	134,428,053
Number of scaffolds	40	92
Number of chromosomes	28	28
Quality Value (QV)	38.9	47.7
Annotated protein-coding genes	18,775	19,752

***BUSCO Assembly and Annotation Completeness Statistics (based on Vertebrate core BUSCOs) and Annotation BUSCO scores***

BUSCO category	Assembly	Annotation	Assembly	Annotation
Complete genes	91.6%	97.2	94.2%	97.9%
Complete + fragmented	95.4%	97.7	96.7%	98.2%
Missing	4.10%	1.3%	2.8%	0.7%
Duplicated	0.5%	1.0%	0.5%	1.1%

672  
673

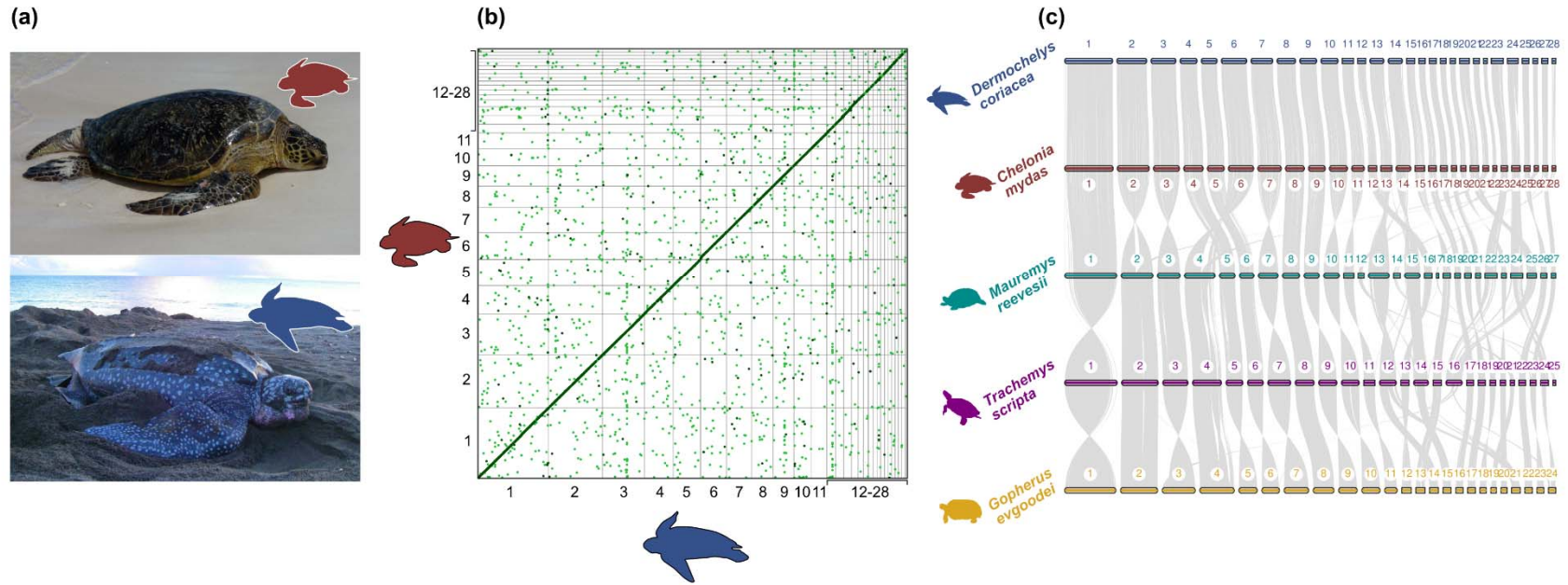


**Fig. 1** | (a) Photographs of green turtle (*Chelonia mydas*); photo credit: NOAA NMFS PIFSC under USFWS Permit #TE-72088A-3, and leatherback turtle (*Dermochelys coriacea*); photo credit: Ricardo Tapilatu. (b) Dot plot showing regions with an identity greater than 0.5 across the entire genomes of green (red) and leatherback (blue) turtles. (c) Gene synteny and collinearity per chromosome among five species of turtles: leatherback turtle (blue), green turtle (red), Chinese pond turtle (*Mauremys reevesii*; green), pond slider turtle (*Trachemys scripta*; purple) and Goode's thornscrub tortoise (*Gopherus evgoodei*; yellow). Each bar represents chromosomes with respective numbers and gray lines represent homolog gene connections among species.

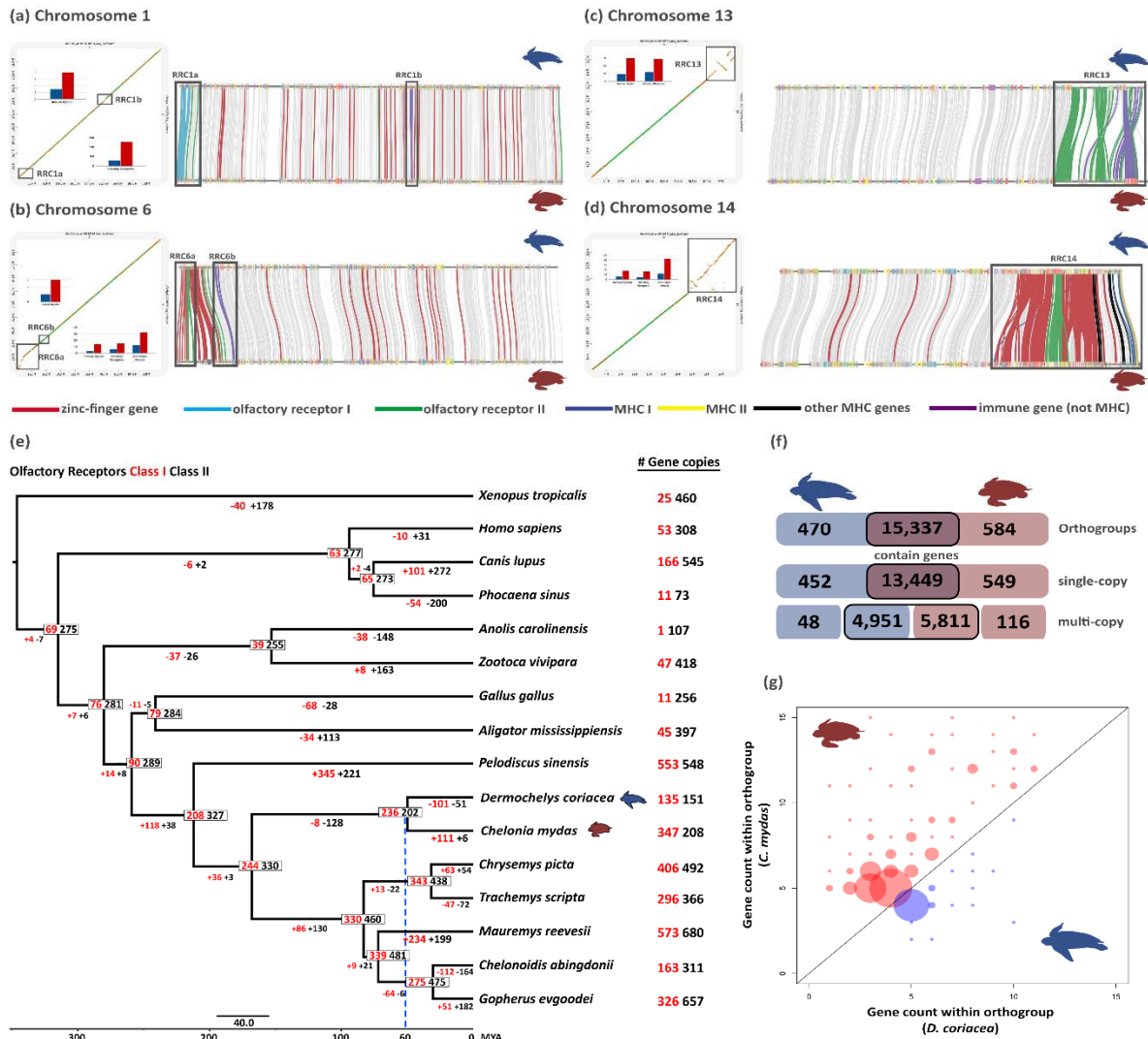


**Fig. 2 | (a-d)** Dotplots (identity values as color; dark green=1-0.75, green=0.75-0.5, orange=0.5-0.25 and yellow=0.25-0) depicting four of the regions with reduced collinearity (RRC) identified within chromosomes and associated with higher copy numbers of immune system, olfactory receptor, or zinc finger domain genes in the green turtle (*Chelonia mydas*) relative to leatherback (*Dermochelys coriacea*) turtle (see also Fig. S3, Tables S3 & S5 for full details of all RRCs). Positions of each RRC are marked with gray squares on the dot plots (left) and gene collinearity maps (right) for each chromosome highlighting the connections among specific gene families in different colors. **(e)** Gene family evolution of olfactory receptors Class I (red) and Class II (black) for amniote phylogeny. Gene numbers are presented on the nodes and gain/loss along each branch are presented below branches. Small scale bar represents substitutions/site and big scale bar represents divergence times (MA). The blue dashed line shows the estimated divergence between the two sea turtle families. **(f)** Number of unique and shared orthogroups and single and multi-copy genes between the two sea turtles (coding genes including genes with rearrangement). The boxes outlined in black denote shared orthogroups, with the higher multi-copy in the green turtle due to greater gene copies within orthogroups. **(g)** Comparison of gene counts between both species per multigenic orthogroup, depicting only those orthogroups where both species have different numbers of genes and a minimum number of five genes for one of the species. Bubbles above the diagonal represent higher counts for the green turtle and below for the leatherback turtle. The size of the bubbles represents the number of orthogroups with the same gene count combination.

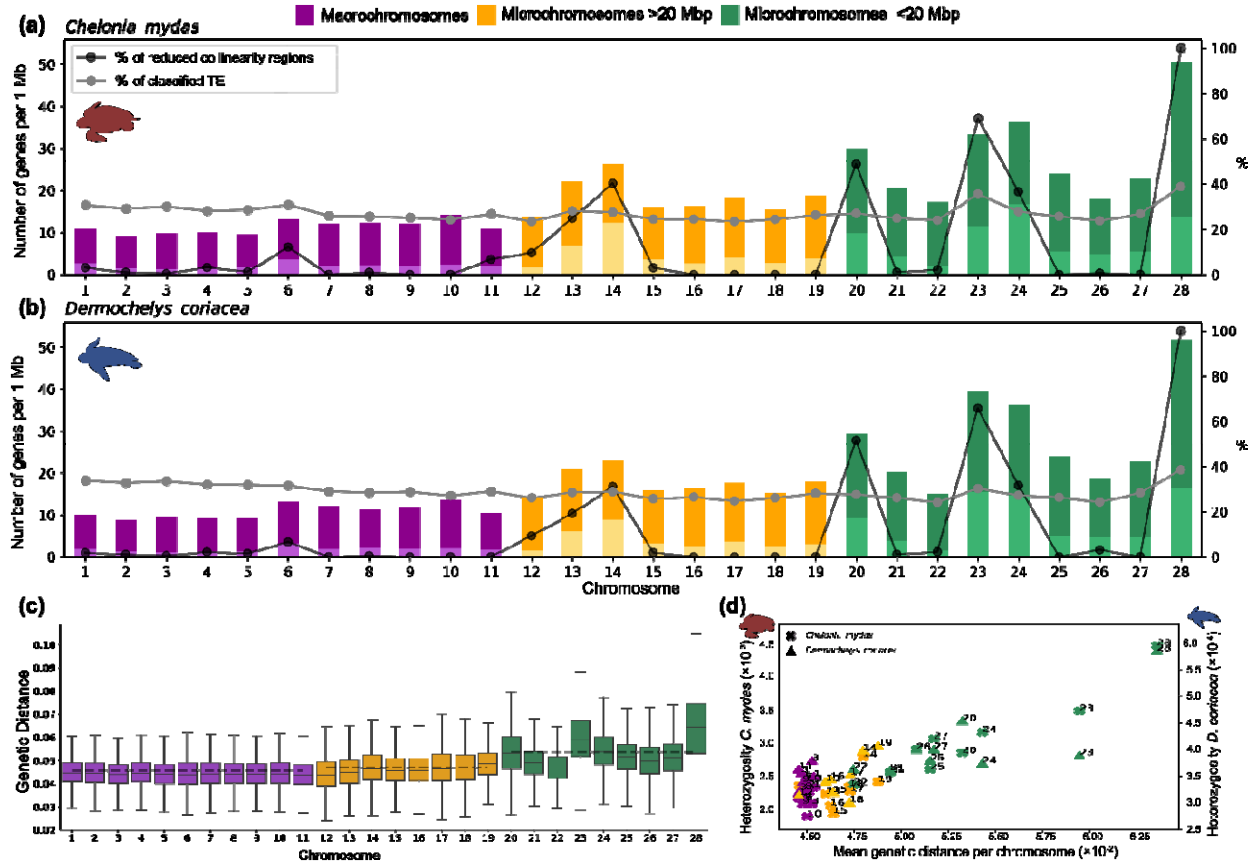


**Fig. 3** | Number of genes, genetic distance between species and heterozygosity within species in macrochromosomes, small (<20 Mb) and intermediate (>20 Mb) microchromosomes. **(a)** Relation between the number of genes, percentage of reduced collinearity regions (RRCs), and classified TE per chromosome for the green (*Chelonia mydas*) and **(b)** leatherback (*Dermochelys coriacea*) turtles. Dark colors indicate to the total number of genes and light colors indicate to the number of multicopy genes. **(c)** Average genetic distance between green and leatherback turtles per chromosome. **(d)** Relation between genetic distance and heterozygosity per chromosome for each species.

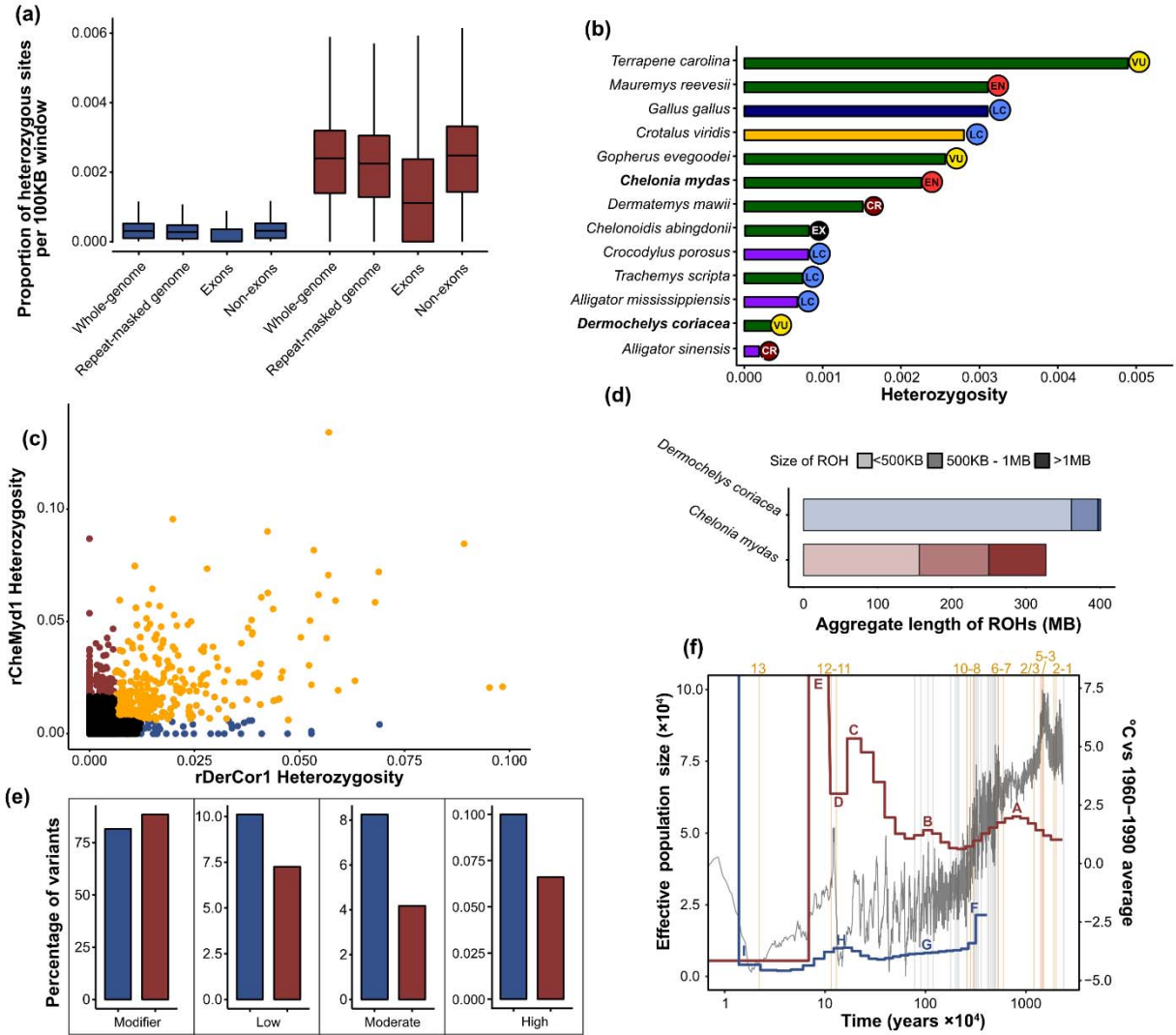


**Fig. 4** | Data is presented for the leatherback (*Dermodochelys coriacea*; blue) and green (*Chelonia mydas*, red) turtle genomes. **(a)** estimates of heterozygosity across the genome calculated with 100 Kb non-overlapping windows for the entire genome, repeat-masked genome, exons and non-exon regions. **(b)** comparison of genome-wide diversity ( $\pi$ ) between the two sea turtle species and 11 other reptile species of varying conservation status using a standardized pipeline for heterozygosity estimation. Bars are colored by taxonomic groups: testudines (green), avians (blue), squamates (yellow), and crocodylians (purple). **(c)** Correlation between heterozygosity in 100 Kb windows containing only exons, generated through alignment to a common reference genome. Windows with higher than mean diversity in leatherbacks (blue), higher in greens (red), and generally high diversity (orange) are highlighted. **(d)** accumulated lengths of runs of homozygosity (ROH). **(e)** predicted impacts of variants from within coding regions. **(f)** Pairwise sequential Markovian coalescent plot (PSMC) of demographic history of both species using a mutation rate of  $1.2 \times 10^{-8}$  and generation time of 30 years, overlaid with temperature (dark grey), magnetic reversals (light grey vertical lines), and selected geological events (orange vertical lines) numbered above as follows: 1. Tethys Sea connectivity changes; 2. [Tethys Sea closure]; 3. [Panama deep water channels close]/Antarctic ice cap starts to grow; 4. Middle Miocene disruption; 5. East Antarctic ice sheet growth; 6. Strait of Gibraltar closes; 7. Zanclean Flood/land bridge between Alaska and Siberia floods; 8. Greenland ice cap starts to grow; 9. Isthmus of Panama formation; 10. Quaternary ice age begins; 11. Onset of Last Glacial Period; 13. Last Glacial Maximum. Repeated numbers/events in square brackets denote uncertainty in timing. Letters indicating portions of the PSMC curves (A-I) are referred to in the text. Data sources are given in supplementary material.

## References

1. R. Hirayama, Oldest known sea turtle. *Nature* **392**, 705–708 (1998).
2. H. B. Shaffer, E. McCartney-Melstad, T. J. Near, G. G. Mount, P. Q. Spinks, Phylogenomic analyses of 539 highly informative loci dates a fully resolved time tree for the major clades of living turtles (Testudines). *Mol. Phylogenet. Evol.* **115**, 7–15 (2017).
3. D. A. Pike, Climate influences the global distribution of sea turtle nesting: Sea turtle nesting distributions. *Glob. Ecol. Biogeogr.* **22**, 555–566 (2013).
4. R. C. Thomson, P. Q. Spinks, H. B. Shaffer, A global phylogeny of turtles reveals a burst of climate-associated diversification on continental margins. *Proc. Natl. Acad. Sci. U. S. A.* **118**, e2012215118 (2021).
5. J. Davenport, Temperature and the life-history strategies of sea turtles. *J. Therm. Biol.* **22**, 479–488 (1997).
6. W. Frair, R. G. Ackman, N. Mrosovsky, Body Temperature of *Dermochelys coriacea*: Warm Turtle from Cold Water. *Science* **177**, 791–793 (1972).
7. P. C. H. Pritchard, “Evolution, Phylogeny, and Current Status” in *The Biology of Sea Turtles*, P. L. Lutz, J. A. Musick, Eds. (CRC Press, 1996), pp. 1–28.
8. L. McClenachan, J. B. C. Jackson, M. J. H. Newman, Conservation implications of historic sea turtle nesting beach loss. *Front. Ecol. Environ.* **4**, 290–296 (2006).
9. J. B. Jackson, *et al.*, Historical overfishing and the recent collapse of coastal ecosystems. *Science* **293**, 629–637 (2001).
10. M. A. Grassman, D. W. Owens, J. P. McVey, R. M. M. Olfactory-based orientation in artificially imprinted sea turtles. *Science* **224**, 83–84 (1984).
11. K. J. Lohmann, C. M. F. Lohmann, There and back again: natal homing by magnetic navigation in sea turtles and salmon. *J. Exp. Biol.* **222**, jeb184077 (2019).
12. P. S. Tomillo, V. S. Saba, R. Piedra, F. V. Paladino, J. R. Spotila, Effects of illegal harvest of eggs on the population decline of leatherback turtles in Las Baulas Marine National Park, Costa Rica. *Conserv. Biol.* **22**, 1216–1224 (2008).
13. S. Fossette, *et al.*, Pan-atlantic analysis of the overlap of a highly migratory species, the leatherback turtle, with pelagic longline fisheries. *Proc. Biol. Sci.* **281**, 20133065 (2014).
14. Y. Kaska, *et al.*, Natural and anthropogenic factors affecting the nest-site selection of Loggerhead Turtles, *Caretta caretta*, on Dalaman-Sarigerme beach in South-west Turkey: (Reptilia: Cheloniidae). *Zool. Middle East* **50**, 47–58 (2010).
15. B. Von Holle, *et al.*, Effects of future sea level rise on coastal habitat. *Journal of Wildlife Management* **83**, 694–704 (2019).
16. N. Mrosovsky, G. D. Ryan, M. C. James, Leatherback turtles: the menace of plastic. *Mar. Pollut. Bull.* **58**, 287–289 (2009).

17. M. Chaloupka, G. H. Balazs, T. M. Work, Rise and fall over 26 years of a marine epizootic in Hawaiian green sea turtles. *J. Wildl. Dis.* **45**, 1138–1142 (2009).
18. L. A. Hawkes, A. C. Broderick, M. H. Godfrey, B. J. Godley, Climate change and marine turtles. *Endanger. Species Res.* **7**, 137–154 (2009).
19. B. P. Wallace, *et al.*, Global conservation priorities for marine turtles. *PLoS One* **6**, e24510 (2011).
20. C. L. Yntema, N. Mrosovsky, Incubation temperature and sex ratio in hatchling loggerhead turtles: a preliminary report. *Mar. Turtle Newsl.* **11**, 9–10 (1979).
21. M. P. Jensen, *et al.*, Environmental Warming and Feminization of One of the Largest Sea Turtle Populations in the World. *Curr. Biol.* **28**, 154–159.e4 (2018).
22. A. D. Mazaris, G. Schofield, C. Gkazinou, V. Almpanidou, G. C. Hays, Global sea turtle conservation successes. *Sci Adv* **3**, e1600730 (2017).
23. IUCN, The IUCN Red List of Threatened Species (2021) (April 16, 2021).
24. L. S. Martínez, *et al.*, Conservation and Biology of the Leatherback Turtle in the Mexican Pacific. *Chelonian Conserv. Biol.* **6**, 70–78 (2007).
25. P. Santidrián Tomillo, *et al.*, Reassessment of the leatherback turtle (*Dermochelys coriacea*) nesting population at Parque Nacional Marino Las Baulas, Costa Rica: effects of conservation efforts. *Chelonian Conserv. Biol.* **6**, 54–62 (2007).
26. J. R. Spotila, R. D. Reina, A. C. Steyermark, P. T. Plotkin, F. V. Paladino, Pacific leatherback turtles face extinction. *Nature* **405**, 529–530 (2000).
27. Laúd OPO Network, Enhanced, coordinated conservation efforts required to avoid extinction of critically endangered Eastern Pacific leatherback turtles. *Sci. Rep.* **10**, 4772 (2020).
28. E. Chan, H. Liew, Decline of the leatherback population in Terengganu, Malaysia, 1956-1995. *Chelonian Conserv. Biol.* **2**, 196–203 (1996).
29. K. L. Eckert, B. P. Wallace, J. G. Frazier, S. A. Eckert, P. C. H. Pritchard, “Synopsis of the biological data on the leatherback sea turtle, *Dermochelys coriacea*” (U.S. Department of Interior, Fish and Wildlife Service, 2012).
30. K. Jones, E. Ariel, G. Burgess, M. Read, A review of fibropapillomatosis in Green turtles (*Chelonia mydas*). *Vet. J.* **212**, 48–57 (2016).
31. G. Zhang, *et al.*, Comparative genomics reveals insights into avian genome evolution and adaptation. *Science* **346**, 1311–1320 (2014).
32. I. Khan, *et al.*, Olfactory Receptor Subgenomes Linked with Broad Ecological Adaptations in Sauropsida. *Mol. Biol. Evol.* **32**, 2832–2843 (2015).
33. D. Jebb, *et al.*, Six reference-quality genomes reveal evolution of bat adaptations. *Nature* **583**, 578–584 (2020).
34. B. J. McMahon, E. C. Teeling, J. Höglund, How and why should we implement genomics into conservation? *Evolutionary Applications* **7**, 999–1007 (2014).

35. M. A. Supple, B. Shapiro, Conservation of biodiversity in the genomics era. *Genome Biol.* **19**, 131 (2018).
36. P. Brandies, E. Peel, C. J. Hogg, K. Belov, The Value of Reference Genomes in the Conservation of Threatened Species. *Genes* **10**, 864 (2019).
37. P. A. Hohenlohe, W. C. Funk, O. P. Rajora, Population genomics for wildlife conservation and management. *Mol. Ecol.* (2020) <https://doi.org/10.1111/mec.15720>.
38. X. Zhang, J. Goodsell, R. B. Norgren Jr, Limitations of the rhesus macaque draft genome assembly and annotation. *BMC Genomics* **13**, 206 (2012).
39. A. Rhie, *et al.*, Towards complete and error-free genome assemblies of all vertebrate species. *Nature* **592**, 737–746 (2021).
40. A. P. Fuentes-Pardo, D. E. Ruzzante, Whole-genome sequencing approaches for conservation biology: Advantages, limitations and practical recommendations. *Mol. Ecol.* **26**, 5369–5406 (2017).
41. Z. Wang, *et al.*, The draft genomes of soft-shell turtle and green sea turtle yield insights into the development and evolution of the turtle-specific body plan. *Nat. Genet.* **45**, 701–706 (2013).
42. A. Whibley, J. L. Kelley, S. R. Narum, The changing face of genome assemblies: Guidance on achieving high-quality reference genomes. *Mol. Ecol. Resour.* **21**, 641–652 (2021).
43. V. Peona, *et al.*, Identifying the causes and consequences of assembly gaps using a multiplatform genome assembly of a bird-of-paradise. *Mol. Ecol. Resour.* **21**, 263–286 (2021).
44. Y. Yuan, *et al.*, Comparative genomics provides insights into the aquatic adaptations of mammals. *Proc. Natl. Acad. Sci. U. S. A.* **118** (2021).
45. N. J. Gemmell, *et al.*, The tuatara genome reveals ancient features of amniote evolution. *Nature* **584**, 403–409 (2020).
46. R. N. Johnson, *et al.*, Adaptation and conservation insights from the koala genome. *Nat. Genet.* **50**, 1102–1111 (2018).
47. J.-N. Hubert, T. Zerjal, F. Hospital, Cancer- and behavior-related genes are targeted by selection in the Tasmanian devil (*Sarcophilus harrisii*). *PLoS One* **13**, e0201838 (2018).
48. L. M. Zimmerman, The reptilian perspective on vertebrate immunity: 10 years of progress. *J. Exp. Biol.* **223**, jeb214171 (2020).
49. H. Lee, J. Gurtowski, S. Yoo, M. Nattestad, S. Marcus, Third-generation sequencing and the future of genomics. *BioRxiv* (2016).
50. M. Seppey, M. Manni, E. M. Zdobnov, BUSCO: Assessing Genome Assembly and Annotation Completeness. *Methods Mol. Biol.* **1962**, 227–245 (2019).
51. G. I. M. Pasquesi, *et al.*, Squamate reptiles challenge paradigms of genomic repeat element evolution set by birds and mammals. *Nat. Commun.* **9**, 2774 (2018).
52. D. Kordis, Transposable elements in reptilian and avian (sauropsida) genomes. *Cytogenet. Genome Res.* **127**, 94–111 (2009).



53. V. Quesada, *et al.*, Giant tortoise genomes provide insights into longevity and age-related disease. *Nat Ecol Evol* **3**, 87–95 (2019).
54. Q.-H. Wan, *et al.*, Genome analysis and signature discovery for diving and sensory properties of the endangered Chinese alligator. *Cell Res.* **23**, 1091–1105 (2013).
55. P. A. Morin, *et al.*, Reference genome and demographic history of the most endangered marine mammal, the vaquita. *Mol. Ecol. Resour.* **21**, 1008–1020 (2021).
56. J. A. Robinson, *et al.*, Genomic Flatlining in the Endangered Island Fox. *Curr. Biol.* **26**, 1183–1189 (2016).
57. P. D. Waters, *et al.*, Microchromosomes are building blocks of bird, reptile, and mammal chromosomes. *Proc. Natl. Acad. Sci. U. S. A.* **118** (2021).
58. C. S. Endres, K. J. Lohmann, Detection of coastal mud odors by loggerhead sea turtles: a possible mechanism for sensing nearby land. *Mar. Biol.* **160**, 2951–2956 (2013).
59. C. S. Endres, N. F. Putman, K. J. Lohmann, Perception of airborne odors by loggerhead sea turtles. *J. Exp. Biol.* **212**, 3823–3827 (2009).
60. M. Manton, A. Karr, D. W. Ehrenfeld, Chemoreception in the migratory sea turtle, *Chelonia mydas*. *Biol. Bull.* **143**, 184–195 (1972).
61. C. Kitayama, *et al.*, Behavioral effects of scents from male mature Rathke glands on juvenile green sea turtles (*Chelonia mydas*). *J. Vet. Med. Sci.* **82**, 1312–1315 (2020).
62. C. S. Endres, *et al.*, Multi-Modal Homing in Sea Turtles: Modeling Dual Use of Geomagnetic and Chemical Cues in Island-Finding. *Front. Behav. Neurosci.* **10**, 19 (2016).
63. K. L. Dodge, J. M. Logan, M. E. Lutcavage, Foraging ecology of leatherback sea turtles in the Western North Atlantic determined through multi-tissue stable isotope analyses. *Mar. Biol.* **158**, 2813–2824 (2011).
64. K. E. Arthur, M. C. Boyle, C. J. Limpus, Ontogenetic changes in diet and habitat use in green sea turtle (*Chelonia mydas*) life history. *Mar. Ecol. Prog. Ser.* **362**, 303–311 (2008).
65. J. A. Seminoff, *et al.*, Large-scale patterns of green turtle trophic ecology in the eastern Pacific Ocean. *Ecosphere* **12**, e03479 (2021).
66. C. Kitayama, *et al.*, Morphological features of the nasal cavities of hawksbill, olive ridley, and black sea turtles: Comparative studies with green, loggerhead and leatherback sea turtles. *PLoS One* **16**, e0250873 (2021).
67. D. Kondoh, C. Kitayama, Y. K. Kawai, The nasal cavity in sea turtles: adaptation to olfaction and seawater flow. *Cell Tissue Res.* **383**, 347–352 (2021).
68. Y. Yamaguchi, *et al.*, Computed tomographic analysis of internal structures within the nasal cavities of green, loggerhead and leatherback sea turtles. *Anat. Rec.* **304**, 584–590 (2021).
69. Y. Niimura, M. Nei, Evolutionary dynamics of olfactory and other chemosensory receptor genes in vertebrates. *J. Hum. Genet.* **51**, 505–517 (2006).

70. L. R. Yohe, M. Fabbri, M. Hanson, B.-A. S. Bhullar, Olfactory receptor gene evolution is unusually rapid across Tetrapoda and outpaces chemosensory phenotypic change. *Curr. Zool.* **66**, 505–514 (2020).
71. H. Saito, Q. Chi, H. Zhuang, H. Matsunami, J. D. Mainland, Odor coding by a Mammalian receptor repertoire. *Sci. Signal.* **2**, ra9 (2009).
72. M. W. Vandewege, *et al.*, Contrasting Patterns of Evolutionary Diversification in the Olfactory Repertoires of Reptile and Bird Genomes. *Genome Biol. Evol.* **8**, 470–480 (2016).
73. A. Liu, *et al.*, Convergent degeneration of olfactory receptor gene repertoires in marine mammals. *BMC Genomics* **20**, 977 (2019).
74. M. A. Constantino, M. Salmon, Role of chemical and visual cues in food recognition by leatherback posthatchlings (*Dermochelys coriacea* L). *Zoology* **106**, 173–181 (2003).
75. H. V. Siddle, J. Marzec, Y. Cheng, M. Jones, K. Belov, MHC gene copy number variation in Tasmanian devils: implications for the spread of a contagious cancer. *Proc. Biol. Sci.* **277**, 2001–2006 (2010).
76. L. E. Escobar, *et al.*, A global map of suitability for coastal *Vibrio cholerae* under current and future climate conditions. *Acta Trop.* **149**, 202–211 (2015).
77. L. Zhang, *et al.*, Massive expansion and functional divergence of innate immune genes in a protostome. *Sci. Rep.* **5**, 8693 (2015).
78. J. P. Elbers, S. S. Taylor, Others, Major histocompatibility complex polymorphism in reptile conservation. *Herpetol. Conserv. Biol.* **11**, 1–12 (2016).
79. X. Vekemans, *et al.*, Whole-genome sequencing and genome regions of special interest: Lessons from major histocompatibility complex, sex determination, and plant self-incompatibility. *Mol. Ecol.* **30**, 6072–6086 (2021).
80. T. Rhen, A. Schroeder, Molecular mechanisms of sex determination in reptiles. *Sex Dev.* **4**, 16–28 (2010).
81. M. Czerwinski, A. Natarajan, L. Barske, L. L. Looger, B. Capel, A timecourse analysis of systemic and gonadal effects of temperature on sexual development of the red-eared slider turtle *Trachemys scripta elegans*. *Dev. Biol.* **420**, 166–177 (2016).
82. H. Merchant-Larios, V. Díaz-Hernández, A. Marmolejo-Valencia, Gonadal morphogenesis and gene expression in reptiles with temperature-dependent sex determination. *Sex Dev.* **4**, 50–61 (2010).
83. T. Wibbels, “Critical Approaches to Sex Determination in Sea Turtles” in *Biology of Sea Turtles*, P. L. Lutz, J. A. Musick, J. Wyneken, Eds. (CRC Press, 2003), pp. 103–134.
84. B. P. Bentley, J. L. Stubbs, S. D. Whiting, N. J. Mitchell, Variation in thermal traits describing sex determination and development in Western Australian sea turtle populations. *Funct. Ecol.* **34**, 2302–2314 (2020).
85. M. Hamann, *et al.*, Global research priorities for sea turtles: informing management and conservation in the 21st century. *Endanger. Species Res.* **11**, 245–269 (2010).

86. J. J. Bull, Sex Determination in Reptiles. *Q. Rev. Biol.* **55**, 3–21 (1980).
87. H. Endoh, N. Okada, Total DNA transcription in vitro: a procedure to detect highly repetitive and transcribable sequences with tRNA-like structures. *Proc. Natl. Acad. Sci. U. S. A.* **83**, 251–255 (1986).
88. M. Kajikawa, K. Ohshima, N. Okada, Determination of the entire sequence of turtle CR1: the first open reading frame of the turtle CR1 element encodes a protein with a novel zinc finger motif. *Mol. Biol. Evol.* **14**, 1206–1217 (1997).
89. C. G. Sotero-Caio, R. N. Platt 2nd, A. Suh, D. A. Ray, Evolution and Diversity of Transposable Elements in Vertebrate Genomes. *Genome Biol. Evol.* **9**, 161–177 (2017).
90. H. B. Shaffer, *et al.*, The western painted turtle genome, a model for the evolution of extreme physiological adaptations in a slowly evolving lineage. *Genome Biol.* **14**, R28 (2013).
91. M. Tollis, *et al.*, The Agassiz’s desert tortoise genome provides a resource for the conservation of a threatened species. *PLoS One* **12**, e0177708 (2017).
92. Z. Wang, T. Miyake, S. V. Edwards, C. T. Amemiya, Tuatara (*Sphenodon*) genomics: BAC library construction, sequence survey, and application to the DMRT gene family. *J. Hered.* **97**, 541–548 (2006).
93. C. Moritz, Strategies to protect biological diversity and the evolutionary processes that sustain it. *Syst. Biol.* **51**, 238–254 (2002).
94. P. Fernandez-Fournier, J. M. M. Lewthwaite, A. Ø. Mooers, Do We Need to Identify Adaptive Genetic Variation When Prioritizing Populations for Conservation? *Conserv. Genet.* **22**, 205–216 (2021).
95. Y. J. Borrell, *et al.*, Heterozygosity-fitness correlations in the gilthead sea bream *Sparus aurata* using microsatellite loci from unknown and gene-rich genomic locations. *J. Fish Biol.* **79**, 1111–1129 (2011).
96. J. A. DeWoody, A. M. Harder, S. Mathur, J. R. Willoughby, The long-standing significance of genetic diversity in conservation. *Mol. Ecol.* **30**, 4147–4154 (2021).
97. Y. Willi, *et al.*, Conservation genetics as a management tool: The five best-supported paradigms to assist the management of threatened species. *Proc. Natl. Acad. Sci. U. S. A.* **119** (2022).
98. L. M. Komoroske, *et al.*, A versatile Rapture (RAD-Capture) platform for genotyping marine turtles. *Mol. Ecol. Resour.* **19**, 497–511 (2019).
99. P. H. Dutton, B. W. Bowen, D. W. Owens, A. Barragan, S. K. Davis, Global phylogeography of the leatherback turtle (*Dermochelys coriacea*). *J. Zool.* **248**, 397–409 (1999).
100. J. Romiguier, *et al.*, Comparative population genomics in animals uncovers the determinants of genetic diversity. *Nature* **515**, 261–263 (2014).
101. M. V. Westbury, B. Petersen, E. Garde, M. P. Heide-Jørgensen, E. D. Lorenzen, Narwhal Genome Reveals Long-Term Low Genetic Diversity despite Current Large Abundance Size. *iScience* **15**, 592–599 (2019).

102. J. A. Robinson, *et al.*, Genomic signatures of extensive inbreeding in Isle Royale wolves, a population on the threshold of extinction. *Sci Adv* **5**, eaau0757 (2019).
103. United States National Marine Fisheries Service, U.S. Fish and Wildlife Service, “Endangered Species Act status review of the leatherback turtle (*Dermochelys coriacea*)” (United States National Marine Fisheries Service, 2020).
104. M. P. Jensen, *et al.*, The evolutionary history and global phylogeography of the green turtle (*Chelonia mydas*). *J. Biogeogr.* **46**, 860–870 (2019).
105. Y. Tikochinski, *et al.*, Mitochondrial DNA short tandem repeats unveil hidden population structuring and migration routes of an endangered marine turtle. *Aquat. Conserv.* (2018) <https://doi.org/10.1002/aqc.2908>.
106. P. J. Bradshaw, *et al.*, Defining conservation units with enhanced molecular tools to reveal fine scale structuring among Mediterranean green turtle rookeries. *Biological Conservation* **222**, 253–260 (2018).
107. M. Kardos, *et al.*, The crucial role of genome-wide genetic variation in conservation. *Proc. Natl. Acad. Sci. U. S. A.* **118**, e2104642118 (2021).
108. P. Dobrynin, *et al.*, Genomic legacy of the African cheetah, *Acinonyx jubatus*. *Genome Biol.* **16**, 277 (2015).
109. A. L. K. Mattila, *et al.*, High genetic load in an old isolated butterfly population. *Proc. Natl. Acad. Sci. U. S. A.* **109**, E2496–505 (2012).
110. M. V. Westbury, *et al.*, Extended and Continuous Decline in Effective Population Size Results in Low Genomic Diversity in the World’s Rarest Hyena Species, the Brown Hyena. *Molecular Biology and Evolution* **35**, 1225–1237 (2018).
111. J. A. Robinson, C. Brown, B. Y. Kim, K. E. Lohmueller, R. K. Wayne, Purging of Strongly Deleterious Mutations Explains Long-Term Persistence and Absence of Inbreeding Depression in Island Foxes. *Curr. Biol.* **28**, 3487–3494.e4 (2018).
112. Y. Xue, *et al.*, Mountain gorilla genomes reveal the impact of long-term population decline and inbreeding. *Science* **348**, 242–245 (2015).
113. A. D. Foote, *et al.*, Killer whale genomes reveal a complex history of recurrent admixture and vicariance. *Mol. Ecol.* **28**, 3427–3444 (2019).
114. N. Dussex, *et al.*, Population genomics of the critically endangered kākāpō. *Cell Genomics* **1**, 100002 (2021).
115. C. C. Kyriazis, R. K. Wayne, K. E. Lohmueller, Strongly deleterious mutations are a primary determinant of extinction risk due to inbreeding depression. *Evol Lett* **5**, 33–47 (2021).
116. Y. D. Dewoody, J. A. Dewoody, On the estimation of genome-wide heterozygosity using molecular markers. *J. Hered.* **96**, 85–88 (2005).
117. J. P. van der Zee, *et al.*, The population genomic structure of green turtles (*Chelonia mydas*) suggests a warm-water corridor for tropical marine fauna between the Atlantic and Indian oceans during the last interglacial. *Heredity* **127**, 510–521 (2021).

118. R. R. Fitak, S. Johnsen, Green sea turtle (*Chelonia mydas*) population history indicates important demographic changes near the mid-Pleistocene transition. *Mar. Biol.* **165**, 110 (2018).
119. S. T. Vilaça, *et al.*, Divergence and hybridization in sea turtles: Inferences from genome data show evidence of ancient gene flow between species. *Mol. Ecol.* (2021) <https://doi.org/10.1111/mec.16113>.
120. A. H. Patton, *et al.*, Contemporary Demographic Reconstruction Methods Are Robust to Genome Assembly Quality: A Case Study in Tasmanian Devils. *Mol. Biol. Evol.* **36**, 2906–2921 (2019).
121. A. Khan, *et al.*, Genomic evidence for inbreeding depression and purging of deleterious genetic variation in Indian tigers. *Proc. Natl. Acad. Sci. U. S. A.* **118** (2021).
122. N. A. O’Leary, *et al.*, Reference sequence (RefSeq) database at NCBI: current status, taxonomic expansion, and functional annotation. *Nucleic Acids Res.* **44**, D733–45 (2016).
123. K. D. Pruitt, *et al.*, RefSeq: an update on mammalian reference sequences. *Nucleic Acids Res.* **42**, D756–63 (2014).
124. F. Cabanettes, C. Klopp, D-GENIES: dot plot large genomes in an interactive, efficient and simple way. *PeerJ* **6**, e4958 (2018).
125. M. Blum, *et al.*, The InterPro protein families and domains database: 20 years on. *Nucleic Acids Res.* **49**, D344–D354 (2021).
126. H. Mi, *et al.*, PANTHER version 16: a revised family classification, tree-based classification tool, enhancer regions and extensive API. *Nucleic Acids Res.* **49**, D394–D403 (2021).
127. B. Paten, *et al.*, Cactus graphs for genome comparisons. *J. Comput. Biol.* **18**, 469–481 (2011).
128. J. Armstrong, *et al.*, Progressive Cactus is a multiple-genome aligner for the thousand-genome era. *Nature* **587**, 246–251 (2020).
129. J. M. Flynn, *et al.*, RepeatModeler2: automated genomic discovery of transposable element families. *Proceedings of the National Academy of Sciences* **117**, 9451–9457 (2020).
130. M. Tarailo-Graovac, N. Chen, Using RepeatMasker to identify repetitive elements in genomic sequences. *Curr. Protoc. Bioinformatics* **Chapter 4**, Unit 4.10 (2009).
131. A. Smit, R. Hubley, P. Green, RepeatMasker Open-4.0. 2013-2015 <http://repeatmasker.org> (2015).
132. F. K. Mendes, D. Vanderpool, B. Fulton, M. W. Hahn, CAFE 5 models variation in evolutionary rates among gene families. *Bioinformatics* (2020) <https://doi.org/10.1093/bioinformatics/btaa1022>.
133. D. M. Emms, S. Kelly, OrthoFinder: solving fundamental biases in whole genome comparisons dramatically improves orthogroup inference accuracy. *Genome Biol.* **16**, 157 (2015).
134. D. M. Emms, S. Kelly, OrthoFinder: phylogenetic orthology inference for comparative genomics. *Genome Biol.* **20**, 238 (2019).
135. G. Hickey, B. Paten, D. Earl, D. Zerbino, D. Haussler, HAL: a hierarchical format for storing and analyzing multiple genome alignments. *Bioinformatics* **29**, 1341–1342 (2013).

136. A. McKenna, *et al.*, The Genome Analysis Toolkit: A MapReduce framework for analyzing next-generation DNA sequencing data. *Genome Res.* **20**, 1297–1303 (2010).
137. H. Li, Aligning sequence reads, clone sequences and assembly contigs with BWA-MEM. *arXiv [q-bio.GN]* (2013).
138. T. S. Korneliussen, A. Albrechtsen, R. Nielsen, ANGSD: Analysis of Next Generation Sequencing Data. *BMC Bioinformatics* **15**, 356 (2014).
139. S. Purcell, *et al.*, PLINK: a tool set for whole-genome association and population-based linkage analyses. *Am. J. Hum. Genet.* **81**, 559–575 (2007).
140. H. Li, R. Durbin, Inference of human population history from individual whole-genome sequences. *Nature* **475**, 493–496 (2011).
141. H. Li, *et al.*, The Sequence Alignment/Map format and SAMtools. *Bioinformatics* **25**, 2078–2079 (2009).
142. H. Li, A statistical framework for SNP calling, mutation discovery, association mapping and population genetical parameter estimation from sequencing data. *Bioinformatics* **27**, 2987–2993 (2011).
143. P. Cingolani, *et al.*, A program for annotating and predicting the effects of single nucleotide polymorphisms, SnpEff: SNPs in the genome of *Drosophila melanogaster* strain w1118; iso-2; iso-3. *Fly* **6**, 80–92 (2012).